

A role for dopamine in the regulation of clock genes: bilateral depletion of endogenous dopamine blunts the rhythm of PER2 expression in the dorsal striatum, the oval nucleus of the bed nucleus of the stria terminalis, and the periventricular nucleus.

Luciana Gravotta

A Thesis
In the Department
of
Psychology

Presented in Partial Fulfillment of the Requirements for the Degree of Master of Arts at
Concordia University
Montreal, Quebec, Canada

August 2010

© Luciana Gravotta, 2010



Library and Archives
Canada

Published Heritage
Branch

395 Wellington Street
Ottawa ON K1A 0N4
Canada

Bibliothèque et
Archives Canada

Direction du
Patrimoine de l'édition

395, rue Wellington
Ottawa ON K1A 0N4
Canada

Your file *Votre référence*
ISBN: 978-0-494-71065-4
Our file *Notre référence*
ISBN: 978-0-494-71065-4

NOTICE:

The author has granted a non-exclusive license allowing Library and Archives Canada to reproduce, publish, archive, preserve, conserve, communicate to the public by telecommunication or on the Internet, loan, distribute and sell theses worldwide, for commercial or non-commercial purposes, in microform, paper, electronic and/or any other formats.

The author retains copyright ownership and moral rights in this thesis. Neither the thesis nor substantial extracts from it may be printed or otherwise reproduced without the author's permission.

AVIS:

L'auteur a accordé une licence non exclusive permettant à la Bibliothèque et Archives Canada de reproduire, publier, archiver, sauvegarder, conserver, transmettre au public par télécommunication ou par l'Internet, prêter, distribuer et vendre des thèses partout dans le monde, à des fins commerciales ou autres, sur support microforme, papier, électronique et/ou autres formats.

L'auteur conserve la propriété du droit d'auteur et des droits moraux qui protègent cette thèse. Ni la thèse ni des extraits substantiels de celle-ci ne doivent être imprimés ou autrement reproduits sans son autorisation.

In compliance with the Canadian Privacy Act some supporting forms may have been removed from this thesis.

While these forms may be included in the document page count, their removal does not represent any loss of content from the thesis.

Conformément à la loi canadienne sur la protection de la vie privée, quelques formulaires secondaires ont été enlevés de cette thèse.

Bien que ces formulaires aient inclus dans la pagination, il n'y aura aucun contenu manquant.


Canada

ABSTRACT

A role for dopamine in the regulation of clock genes: bilateral depletion of endogenous dopamine blunts the rhythm of PER2 expression in the dorsal striatum, the oval nucleus of the bed nucleus of the stria terminalis, and the periventricular nucleus.

Luciana Gravotta

Recent studies have shown that clock genes influence the expression of enzymes involved in the regulation of dopamine levels, and that reciprocally, dopamine signaling can influence the expression of several clock genes. Although many studies have looked at the response of clock genes to increases in dopamine via the use of dopamine agonists or stimulant drugs that affect dopamine release and reuptake, very few have looked at the response to decreases in endogenous dopamine. The present thesis sought to examine the effect of intracerebroventricular (i.c.v.) injection of 6-OHDA on the expression of the clock gene, PERIOD2 (PER2) in the dorsal striatum and the limbic forebrain.

Specifically, PER2 expression was quantified in the suprachiasmatic nucleus (SCN), the dorsal striatum, the oval nucleus of the bed nucleus of the stria terminalis (BNSTov), the central nucleus of the amygdala (CEA), the basolateral amygdala (BLA), and the dentate gyrus (DG); all areas that have been previously shown to express PER2 with circadian rhythmicity. Rats that received i.c.v. 6-OHDA injections showed bilateral depletion of dopamine throughout the basal ganglia and the extended amygdala as well as a blunted rhythm of PER2 expression in the striatum and the BNSTov. A novel rhythm of PER2 expression was observed in the periventricular nucleus of the hypothalamus (PV) of control rats and this rhythm was blunted in 6-OHDA lesioned rats. This interaction

between dopamine and clock gene expression has implications for the study of circadian disruptions in mood disorders and in parkinson's disease.

Table of Contents

	Page
List of Figures.....	vi
Introduction.....	1
Methods.....	15
Results.....	21
Discussion.....	56
References.....	74

LIST OF FIGURES

	Page
Figure 1. Representative double plotted actogram for a sham rat. The numbers indicate the day, starting with day 0 when rats were first placed in the boxes. Vertical marks indicate periods of activity of at least 10 wheel revolutions/10min. White background indicates lights on, grey background indicates lights off. Arrow indicates surgery day.	22
Figure 2. Representative double plotted actogram for a 6-OHDA lesioned rat. The numbers indicate the day, starting with day 0 when rats were first placed in the boxes. Vertical marks indicate periods of activity of at least 10 wheel revolutions/10min. White background indicates lights on, grey background indicates lights off. Arrow indicates surgery day.	23
Figure 3. Representative double plotted actogram for a 6-OHDA lesioned rat. The numbers indicate the day, starting with day 0 when rats were first placed in the boxes. Vertical marks indicate periods of activity of at least 10 wheel revolutions/10min. White background indicates lights on, grey background indicates lights off. Arrow indicates surgery day.	24

Figure 4. Representative double plotted actogram for a 6-OHDA lesioned rat. The numbers indicate the day, starting with day 0 when rats were first placed in the boxes. Vertical marks indicate periods of activity of at least 10 wheel revolutions/10min. White background indicates lights on, grey background indicates lights off. Arrow indicates surgery day. 27

Figure 5. Representative double plotted actogram for a 6-OHDA lesioned rat. The numbers indicate the day, starting with day 0 when rats were first placed in the boxes. Vertical marks indicate periods of activity of at least 10 wheel revolutions/10min. White background indicates lights on, grey background indicates lights off. Arrow indicates surgery day. 28

Figure 6. Representative photomicrographs of TH-ir fibers in the striatum at 5x (A,B) and 20x (C,D) magnification of sham (A,C) and 6-OHDA lesioned (B,D) rats perfused 4 weeks after surgery. 30

Figure 7. Representative photomicrographs of TH-ir fibers in the striatum of a sham rat (A) and a 6-OHDA rat with an uneven lesion (B) perfused 4 weeks after surgery. 31

Figure 8. Stereotaxic maps of areas captured in the striatum. Panels A and B depict the anterior striatum and panels C and D depict the posterior striatum. Yellow areas show the anteromedial striatum, red areas show the

anterolateral striatum, orange areas show the posteromedial striatum, and green areas show the posterodorsal striatum. Arrows show landmarks used to ensure localization of the area. Small grey boxes represent the target area within which the 400x400 picture used for the PER2 analysis was taken (figures modified from Paxinos & Watson, 2004). 33-34

Figure 9. Mean number (\pm SEM) of PER2-ir cells in the anterior medial (A), anterior lateral (B), posterior medial (C), and posterior lateral (D) striatum for sham and 6-OHDA lesioned rats perfused 4 weeks after surgery. n = 6 per time point for the sham group. n = 7 at ZT1 and n = 9 at ZT14 for the 6-OHDA group. 37

Figure 10. Representative photomicrographs of PER2-ir cells in the SCN of a sham (A, top panels) and a 6-OHDA lesioned (B, bottom panels) rat at ZT1 and ZT14. 3V = third ventricle. 39

Figure 11. Mean number (\pm SEM) of PER2-ir cells in the SCN (A), BNSTov (B), BLA (C), CEA (D), and DG (E) of sham and 6-OHDA group rats perfused 4 weeks after surgery. n = 6 per time point for the sham group. n = 7 at ZT1 and n = 9 at ZT14 for the 6-OHDA group. 40

Figure 12. Representative photomicrographs at 10x magnification of PER2-ir cells in the BNSTov of a sham (A, top panels) and a 6-OHDA lesioned rat (B, bottom panels) perfused 4 weeks after surgery at ZT1 and ZT14. 41

Figure 13. Representative photomicrographs at 5x magnification of TH-ir fibers in the BNSTov of a sham rat (A) and a 6-OHDA lesioned rat (B) perfused 4 weeks after surgery. LV = lateral ventricle, AC = anterior commissure. 43

Figure 14. Representative photomicrographs at 10x magnification of TH-ir fibers in the CEA (black circle) of a sham rat (A) and a 6-OHDA lesioned rat (B) perfused 4 weeks post surgery. 44

Figure 15. Mean number (\pm SEM) of PER2-ir cells (A) and TH-ir cells (B) in the periventricular nucleus of sham and 6-OHDA group rats perfused 4 weeks after surgery. n = 6 per time point for the sham group. n = 7 at ZT1 and n = 9 at ZT14 for the 6-OHDA group. 46

Figure 16. Representative photomicrographs at 10x magnification of PER2-ir cells in the PV of a sham (A, top panels) and a 6-OHDA lesioned rat (B, bottom panels) at ZT1 (left panels) and ZT14 (right panels). 3V = third ventricle, PV = periventricular nucleus. 48

Figure 17. Representative photomicrographs of TH-ir cells and fibers in the periventricular nucleus of a sham (left panels) and a 6-OHDA lesioned (right panels) rat at 5x (A, upper panels) and 10x (B, lower panels) magnification 3V = third ventricle, SCN = suprachiasmatic nucleus, PV = periventricular nucleus.

49

Figure 18. Representative photomicrographs at 5x magnification of TH-ir cells and fibers in the SN and in the VTA of a sham rat (A, top panels), a 6-OHDA lesioned rat with a greater depletion (B, middle panels), and a 6-OHDA lesioned rat with a lesser depletion (C, bottom panels) of TH-ir cells and fibers.

52

Figure 19. Representative photomicrographs at 5x magnification of TH-ir cells in the striatum (A), SN (B), VTA (C), Acc (D), BNSTov (E), and CEA (F) for a 6-OHDA lesioned rat with less depletion of TH-ir fibers (left panels) and a 6-OHDA lesioned rat with a larger depletion of TH-ir fibers (right panels)

54-55

INTRODUCTION

Animals exhibit many behaviors and physiological processes that cycle every 24 hours. This circadian rhythm (“circa diem” means “approximately one day”) of behaviors is adaptive in that it tunes an organism to its environment, and thus allows animals to predict important cyclic events (e.g., food availability, emergence of predators), and engage in the appropriate behaviors to optimize their chance of survival (e.g., anticipatory activity such as foraging, retreating into burrows to avoid predators). It seems that internal rhythms have developed due to the inherent cyclic nature of our environment, which gives a competitive advantage to those that can keep track of the time cues in the external environment and execute behaviors at a specific time of day. This can be seen even in simple organisms such as cyanobacteria. Experiments that compare normal cyanobacteria with those that have been mutated so that they exhibit either no rhythm or dampened rhythms show that when both strains are placed in a rhythmic environment (e.g., a rhythm of 12hrs of darkness followed by 12hrs of light) the mutated strains are at a competitive disadvantage. However, if both strains are placed in a constant environment (e.g., 24 hours of constant light) they fare equally well (Woelfle, Ouyang, Phanvijhitsiri, & Johnson, 2004). These results highlight the evolutionary advantage of an internal time-keeping system given changing, yet cyclic, environmental conditions.

In mammals, the central pacemaker in the brain that keeps time for the entire organism is located in the suprachiasmatic nuclei (SCN) of the hypothalamus. Through both neural and diffusible signals, these nuclei coordinate the timing of, amongst others, hormonal, neuroendocrine, and activity rhythms (LeSauter & Silver, 1998). Each cell of

the SCN has its own time-keeping device that consists of autoregulatory positive and negative feedback loops of clock genes and proteins (Reppert & Weaver, 2002; Albrecht, 2006).

With the recent finding that clock genes are widely distributed throughout the brain and periphery (Amir & Stewart, 2009; Hastings, Reddy, & Maywood, 2009) there has been much interest in uncovering the role of clock genes in areas outside of the SCN and in understanding the mechanisms that regulate and synchronize the extra-SCN clocks. The striatum is an area involved in the regulation of voluntary motor movements (Albin, Young, & Penney, 1989; DeLong & Wichmann, 2009) and as discovered more recently, in decision-making (Balleine, Delgado, & Hikosaka, 2007) and affective learning (Delgado, Schiller, & Phelps, 2008). Proper functioning of the striatum critically depends on the dopamine (a neurotransmitter) input that it receives from a group of dopaminergic cells located in the substantia nigra pars compacta (SNc) (Ungerstedt, 1971a). Recently it has been found in the mouse that the striatum exhibits a circadian rhythm of mouse *Per1* (*mPer1*) and *mPer2* levels (Iijima, Nikaido, Akiyama, Moriya, & Shibata, 2002; Manev & Uz, 2006). Furthermore, converging evidence from various fields shows that the local circadian clock in the striatum modulates striatal dopamine, and that this relationship may be reciprocal (Falcon & McClung, 2009). Based on these findings, this work aims to study the impact that dopamine has on clock genes.

The master clock and the semi-autonomous oscillators

Early studies showed that bilateral lesions of the SCN led to the loss of circadian rhythms of both drinking and locomotor behaviors in the rat (Stephan & Zuker, 1972)

and of melatonin (a hormone involved in the regulation of sleep) rhythms in the rhesus monkey (Reppert et al., 1981). Since these initial lesion studies that demonstrated the critical role of the SCN in maintaining circadian rhythms of physiological processes and of behavior, much work has been done to flesh out the details of how this master clock ticks.

Neurons of the SCN are self-sustaining oscillators: studies in which SCN neurons are kept alive in vitro demonstrate that these neurons, in the absence of any input, retain the same rhythmic oscillations of firing rates and of protein synthesis as prior to explantation (Green & Gillette, 1982; Shibata, Hamada, Tominaga, & Watanabe, 1992; Welsh, Logothetis, Meister, & Reppert, 1995). At the level of gene expression, the internal time keeping system of each neuron consists of positive and negative feedback loops which control the transcription and translation of several clock genes. These include the Circadian Locomotor Output Cycles Kaput (CLOCK) gene, the Brain and Muscle Arnt-like protein-1 (BMAL1) gene, the Period (PER1, PER2, and PER3) genes, and the Cryptochrome (CRY1 and CRY2) genes, amongst others (Reppert & Weaver, 2002; Albrecht, 2006). Heterodimers of BMAL1 and CLOCK act as positive regulators by inducing the transcription of *Per* and *Cry* genes. *Per* mRNA and *Cry* mRNA are then transported to the cytoplasm where they undergo translation into their protein products, namely, PER and CRY. Once PER and CRY proteins heterodimerize, they can re-enter the nucleus where they then act upon BMAL1:CLOCK to inhibit the transcription of their own genes (Reppert & Weaver, 2002; Hastings, O'Neill, & Maywood, 2007). One full cycle of the rodent 'clock' takes approximately 24hrs, with the negative regulators (PER

and CRY) peaking at the end of the subjective day (Hastings, O'Neill, & Maywood, 2007).

The self-sustainability of the individual cells and of the master clock itself is reflected in self-sustaining behavioral outputs; when animals are placed in constant conditions such constant darkness, where there are no time cues available, they do not lose their daily cycles of behavioral and physiological outputs. For example, under constant darkness, rats continue to display activity cycles of approximately 24 hours (Meijer, 2001). However, these cycles are usually slightly longer than 24 hours and thus when placed in these conditions, the animal slowly loses its alignment with the solar day (Golombek & Rosenstein, 2010). Entrainment refers to the alignment of the endogenous period of the animal to the exogenous period (i.e., the 24 hour day) and entrainment is achieved with the help of a zeitgeber, an external cue that signals the start of each cycle. Light onset is the most potent zeitgeber for mammals (Reppert & Weaver, 2002) and information about lighting conditions reaches the SCN through the retinohypothalamic tract (RHT) from the retina (Albrecht, 2006). Light induces *Per1* and *Per2* in the SCN, and by this means is able to speed up or slow down the clock thus aiding in entrainment (Reppert & Weaver, 2002; Hastings, O'Neill, & Maywood, 2007). As only the core region of the SCN receives input from the retina, the entrainment signal must be delivered to the shell region of the SCN in order to ensure coordination of all the neurons within the SCN. This is achieved through intercellular signaling; vasoactive intestinal polypeptide (VIP), a neuropeptide found in the core region of the SCN has been found to mediate the synchronization between cells in the two regions (Hastings, O'Neill, & Maywood, 2007).

Beginning in *Drosophila* and then extending to other species, researchers also found that clock genes show rhythmic expression in peripheral organs, but that these rhythms depend on input from the SCN (Hastings, Reddy, & Maywood, 2003). Unlike SCN explants that when kept alive *in vitro* show rhythmic oscillations for weeks, peripheral explants (e.g., liver) show a dampening of the rhythm in just a few days demonstrating that peripheral clocks are not self-sustaining. More recently, it was discovered that specific structures in the limbic forebrain display a rhythmic oscillation of PER2, an essential oscillating component of the clock gene feedback loop. These include the oval nucleus of the bed nucleus of the stria terminalis (BNSTov), the central nucleus of the amygdala (CEA), the basolateral amygdala (BLA), and the hippocampus (HC) (Lamont, Robinson, Stewart & Amir, 2005). The striatum is another area that has recently been found to display rhythmic oscillations of clock genes (Iijima et al., 2002; Uz, Akhisaroglu, Ahmed, & Manev, 2003).

Although these areas ultimately depend on the SCN for rhythmic expression (Amir, Lamont, Robinson, & Stewart, 2004), they are termed semi-autonomous oscillators because their rhythms and synchronization are also sensitive to other signals such as food, stress, hormones, and drug administration (Verwey, Khoja, Stewart, & Amir, 2007; Lamont, Diaz, Barry-Shaw, Stewart, & Amir, 2006; Takahashi et al., 2001; Perrin et al., 2006; Iijima et al., 2002). For example, restricted feeding (i.e., the restricting of food access to a few hours during the day) in rats changes the rhythm of PER2 expression in the BNSTov, CEA, BLA, DG, and dorsomedial hypothalamus (DMH), but does not affect the rhythm of PER2 in the SCN (Verwey, Khoja, Stewart, & Amir, 2007). A similar dissociation was observed in the striatum where daily methamphetamine

injections shifted *mPer1* and *mPer2* expression, but did not change the rhythm of these genes in the SCN (Iijima et al., 2002). Unlike the SCN, the function of these semi-autonomous oscillators is still not well understood (McClung et al., 2005; Lynch et al., 2008). As these areas are important for a wide range of functions such as voluntary movement, emotion, memory, etc., it is important to attempt to uncover the role of clock genes in these regions.

The role of clock genes in dopamine regulation

Several studies provide evidence that clock genes play a role in the regulation of dopamine (DA) levels. Firstly, in the striatum, there is a diurnal rhythm of dopamine, its metabolites, and in the enzymes involved in its production. For example, in the rat, there is a diurnal rhythm of tyrosine hydroxylase (TH, the first step enzyme in catecholamine synthesis) mRNA levels in the substantia nigra and in the ventral tegmental area (VTA) and of D2 receptor mRNA levels in the caudate putamen (Weber, Lauterburg, Tobler, Burgunder, 2003). Interestingly, *Drosophila* without a functional period gene do not display the diurnal variation in D2 receptor observed in wild-type (WT) *Drosophila* (Andretic, Chaney, & Hirsh, 1999). Dopamine itself also displays a diurnal rhythm in the dorsal striatum (Paulson & Robinson, 1994; Castañeda, de Prado, Prieto, & Mora, 2004). Secondly, disruption of clock genes leads to abnormal behavioral and neurophysiological responses to drugs that have an effect on dopamine neurotransmission. For example, *Drosophila* with a mutation of the *period* gene (*per⁰*) do not sensitize to cocaine. Furthermore, exposure to cocaine and subsequent administration of quinpirole (a D2 receptor agonist) does not result in the increased motor response normally elicited in WT

flies. The response observed in WT flies is thought to be mediated by an increase in D2 receptor responsiveness that is absent in *per^o* flies (Andretic, Chaney, & Hirsh, 1999). Studies with mice have shown that *mPer1* mutants, like *Drosophila*, do not show sensitization to cocaine. However, *mPer2* mutant mice show hypersensitization to cocaine when compared to WT mice (Abarca, Albrecht, & Spanagel, 2002). *Clock* mutant mice also display an altered response to cocaine: greater TH expression and greater DA cell firing in the VTA than WT mice (McClung et al., 2005). Finally, Hampp and colleagues have shown that one of the putative mechanisms by which clock genes can control dopamine levels in the striatum is through the regulation of monoamine oxidase A (*maoa*) mRNA expression. MAOA is an enzyme that is involved in the degradation of DA. *Per2* mutant mice show a decrease in *maoa* expression and a resulting increase in DA levels. Furthermore, transcription of *Maoa* is regulated by PER2, BMAL1, and NPAS2 (Hampp et al., 2008).

The aforementioned studies, which demonstrate the role of clock genes in the regulation of DA levels, as well as the established role of DA in addiction (Volkow et al., 2007; Le Foll et al., 2009), suggest that there is a link between clock genes and addiction. There also seems to be a link between clock genes and mood disorders. Roybal and colleagues (2007) have shown that mice with a mutation in the *Clock* gene show behavioral abnormalities resembling mania in humans and that they display an enhanced preference for rewarding stimuli, including cocaine (Roybal et al., 2007). Clinical studies have shown that patients suffering from depression or bipolar disorder (BPD) exhibit blunted or abnormal rhythms of, for example, body temperature, blood pressure, norepinephrine (a catecholamine that can act as a hormone and a neurotransmitter), and

melatonin (McClung, 2007). Although there is a link between mood disorders and the abnormal functioning of the DA system (Nestler & Carlezon, 2006), the link between dopamine, clock genes, and circadian rhythms (in the context of mood disorders) remains to be elucidated (McClung, 2007).

A reciprocal role for dopamine

It is important to note that the relationship between clock genes and dopamine is reciprocal and there is much evidence showing that dopamine can affect clock gene expression. Firstly, developmental research in rats and Syrian hamsters has shown that there is a window of time during which the SCN clock can be entrained by dopamine. During fetal development and up until approximately the fifth day after birth (PD5), dopamine elicits the expression of c-Fos, an immediate early gene and a marker of neuronal activity, in the SCN and can entrain activity rhythms (Weaver & Reppert, 1995; Grosse & Davis 1999). Another line of evidence for dopamine influence comes from research on clock gene expression in retinal photoreceptive cells. In vitro experiments show that dopamine agonists increase expression of *xPer2* in photoreceptor cells in *Xenopus laevis* retina (Besharse, Zhuang, Freeman, & Fogerty, 2004). In the mouse retina, clock gene response to light is mediated by dopamine. Both light and dopamine induce *mPer1* expression in the retina. Yujnovsky and colleagues have shown that the increased expression of *mPer1* in response to a D2R specific dopamine agonist is mediated by the modulatory effect that D2R signaling has on CLOCK:BMAL1 activity (Yujnovsky et al., 2006).

Several studies have linked exposure to drugs of abuse that interfere with normal dopamine metabolism with changes in clock gene expression. Drugs of abuse such as cocaine and methamphetamine can entrain locomotor activity rhythms and have been shown to alter the rhythm of clock gene expression, and in some cases induce or repress the expression of clock genes in the striatum (Yuferov et al., 2003; Manev & Uz, 2006; Kosobud et al., 2007; Lynch et al., 2008).

Hypothalamic Dopamine and the SCN

Clinical studies of patients with Parkinson's Disease (PD), a disorder believed to be caused by the degeneration of dopaminergic neurons in the substantia nigra, suggest that these patients suffer from more sleep disorders than the general population (Dhawan, 2006). Studies have also shown that PD patients treated with L-DOPA (a precursor of dopamine), experience an advance in dim light melatonin onset (DLMO), and based on this evidence, it has been suggested that L-DOPA may induce a phase advance in the sleep-wake cycle (Garcia-Borreguero et al., 2004; Fertl et al., 1993).

Although these clinical findings suggest a possible role for dopamine in the sleep-wake cycle, stronger evidence for the link between dopamine and the master clock comes from animal studies. As previously mentioned, dopamine can entrain the SCN in pre- and peri-natal rodents. The fetuses of a SCN lesioned hamster can be entrained by a daily injection of SKF 38393, a D1 receptor agonist. This treatment also induces c-fos expression in the fetal SCN (Weaver & Reppert 1995). In adult rats, c-fos expression in the SCN is induced by light and correlates with light-mediated shifts in circadian activity rhythms, however, SKF 38393 does not induce c-fos expression in the SCN (Rusak et al.,

1990). Interestingly, this loss of sensitivity to SKF 38393 with age is not due to the loss of D1 receptors. D1 receptor mRNA has been observed in the SCN of the adult rats (Freneau, 1991; Ishida, 2002) and in Siberian hamsters (Duffield, 1998). In primates, Rivkees and colleagues have shown that there is no loss in the levels of D1 receptors as baboons reach adulthood. In humans, the infant brain shows higher levels of D1 receptors than the adult brain, albeit there are still D1 receptors present in the adult brain (Rivkees et al., 1997).

Ishida and colleagues have shown that aromatic L-aminoacid decarboxylase (AADC), a second-step enzyme in the production of monoamines, is present in the SCN and both mRNA levels and enzymatic activity are rhythmic, with a peak early in the day and a trough in the early night. Interestingly, although the SCN contains only sparse DA immunoreactive (ir) fibers, when L-DOPA was administered by intraperitoneal (i.p.) injection, DA-ir cell bodies were observed in the SCN. In parallel to what was observed in PD patients receiving L-DOPA treatment, Ishida and colleagues suggest that the high levels of circulating L-DOPA in the bloodstream could be converted into DA by these cells and this DA could act upon D1 receptors in the SCN to affect its rhythm (Ishida, 2002). However, Ishida and colleagues did not measure locomotor activity rhythms nor clock gene expression in order to determine if there was any effect of L-DOPA loading on SCN rhythms. Yamada and colleagues suggest that activation of SCN D1 receptors does have an effect on locomotor activity rhythms. When rats are placed in constant darkness (DD), systemic treatment with a D2 receptor agonist (4-propyl-9-hydroxynaphthoxazine or PHNO) increases the amplitude of activity rhythms and treatment with a D1 receptor agonist (SKF 38393) lengthens the period of locomotor

activity (Yamada, 1991). The authors suggest that a change in the amplitude need not involve the SC but that a change in the period most likely reflects an effect on the SCN. They thus conclude that systemically administered SKF 38393 stimulates the D1 receptors located in the SCN and leads to a lengthening of the period of locomotor activity.

Unfortunately, no other studies have demonstrated changes in SCN rhythms in response to D1 receptor agonists and very few studies have looked at the direct effect of dopamine on the SCN. One study that used single cell recording to examine the excitatory effect of different neurotransmitters on SCN neurons showed that dopamine excited 50% of SCN neurons in OVX rats and 27.1% in OVX rats that were administered estrogen.

Although the literature on the effect of dopamine on the SCN is scarce, the presence of D1 receptors and AADC in the adult rodent SCN suggests the possibility that dopamine may have a role to play in the SCN. As there are no dopaminergic cells in the SCN (Lindvall, Bjorklund, & Skagerberg 1984; Bjorklund & Nobin, 1973), the question remains as to where dopamine input comes from. One possibility, as suggested by Ishida and colleagues is that precursors to dopamine could travel in the blood stream and then be converted to DA in the SCN (Ishida, 2002). Another possibility is that there may be projections from DAergic neurons to the SCN. The seat of the SCN, the hypothalamus, contains several dopaminergic cell groups (Lindvall, Bjorklund, & Skagerberg, 1984; Bjorklund & Nobin, 1973; van den Pol, Herbst, & Powell, 1984). The rostral periventricular DA cell group (group A14, also known as the periventricular nucleus (PV)) is located in the rostral medial hypothalamus on either side of the third ventricle

and extends from -0.24 to -1.08 (AP) (Bjorklund & Nobin, 1973). As a large portion of this cell group is located immediately dorsal to the SCN and the DA fibers are oriented dorso-ventrally (Lindvall, Bjorklund, & Skagerberg, 1984), this cell group may be a good candidate for DA projections to the SCN. Also, van den Pol and colleagues have observed TH-ir cell bodies in between the two SCN whose dendrites run in the rostro-caudal direction, and they suggest that dendrites from these cells could innervate the SCN.

The preceding studies show that it remains to be elucidated what role, if any, dopamine has in the function of the adult rodent SCN. Furthermore, no studies have looked at whether hypothalamic DAergic neurons, and more specifically, the A14 cell group have an influence on adult rodent SCN functioning.

Rationale and objectives

This study had two main goals. The first was to elucidate whether periventricular hypothalamic dopamine has an influence on the functioning of the master clock by depletion of periventricular hypothalamic dopamine and assessment of the effects of this depletion on locomotor activity rhythms and on PER2 expression in the SCN. The second was to determine the effect of a bilateral depletion of dopamine input to the striatum on the expression and rhythmicity of PER2 in the striatum. The majority of studies that use 6-OHDA create unilateral lesions, and only a few (Borowsky & Kuhn, 1993; Carvey, Lin, Faselis, Notermann, & Ling, 1996; Rodríguez, Barroso-Chinea, Abdala, Obeso & González-Hernández, 2001; Rey et al., 2007) have used the method employed in this study.

Although most of the aforementioned studies show the response of clock genes to increases in dopamine levels, very few studies have looked at the response to decreases in endogenous dopamine. Recently our lab has used the method of unilateral injection of 6-hydroxy dopamine (6-OHDA) into the medial forebrain bundle (MFB) in order to deplete dopaminergic neurons in the substantia nigra pars compacta (SNc) and eliminate dopamine input to the striatum. We have shown that this procedure leads to a reduction in the peak of PER2 expression and a reduction of PER1 expression in the dorsal striatum and in the BNSTov on the side ipsilateral to the lesion. PER2 expression in the SCN, BLA, CE, and HC, however, is not affected by this manipulation (Hood, unpublished results).

The present study aims to expand on these findings by investigating the effect of bilateral dopamine depletion on PER2 expression in the aforementioned areas. Although the unilateral 6-OHDA lesion has been widely favored due to the viability of animals post lesion, the ease of lesion confirmation, and the ability to use the contralateral hemisphere as a control, some issues remain concerning its use. The issue that concerns us most here is whether the unlesioned side can assume a compensatory role, and if so, what effect that would have on what is observed on the lesioned side and how this would affect the function of the unlesioned side. A few studies have shown that there is an increase in extracellular dopamine on the side contralateral to the lesion following a unilateral 6-OHDA lesion (Blum et al., 2001; Gonzalez-Hernandez, Barroso-Chinea, & Rodriguez, 2004) and it has been suggested that as the nigrostriatal systems of both hemispheres show interdependent regulation, the unlesioned side may provide compensation of function for the lesioned side (Roedter et al., 2001). If this is indeed the case, then it is

also possible that with the unilateral model, we are not seeing the full effect of dopamine depletion on clock proteins.

In the present study, we injected 6-OHDA into the third ventricle, directly dorsal to the SCN. The injection location was chosen to target the hypothalamic dopamine neurons surrounding the SCN and in order to obtain bilateral striatal depletion of dopamine. This technique has been previously shown to induce a dose-dependent destruction of dopamine neurons in the substantia nigra and of dopamine input to the striatum (Rodríguez, Barroso-Chinea, Abdala, Obeso & González-Hernández, 2001; Rey et al., 2007). Following the injections, animals were placed in constant darkness for two weeks in order to control for the masking effect that light has on locomotor activity of nocturnal animals, i.e., an overall suppression of locomotor activity (Redlin, 2001), and thus better determine the effect of the lesion on the circadian rhythm of locomotor activity. Animals were then put back on a 12:12 LD schedule in order to determine if re-entrainment is possible after such widespread depletion of dopamine input and dopaminergic neurons. Finally, rats were killed and expression of PER2 and TH was determined using immunohistochemistry.

METHODS

Animals and Housing

Male Wistar rats (Charles River Laboratories, St-Constant, QC) weighing approximately 350 grams on the day of surgery were used in this study. Each rat was housed in a clear plastic cage with a metal grid floor and a running wheel and was given unrestricted access to food and water. All procedures were carried out in accordance with the Canadian Council on Animal Care guidelines and were approved by the Animal Care Committee of Concordia University.

Rats were individually housed in their cages within a ventilated chamber that was light and sound proof and outfitted with a computer-controlled lighting system (VitalView; Mini Mitter Co. Inc, Sunriver, OR, USA). Running wheel revolutions were constantly monitored and recorded with the VitalView system and later analyzed and plotted using Circadia Software (Behavioral Cybernetics, Cambridge, MA).

Procedure

Rats were given approximately two weeks of habituation to the home cage upon arrival. This allowed them to reach the appropriate weight for surgery and to entrain to a 12:12hr LD cycle. Rats were handled for 3 days prior to surgery. Prior to handling, rats were randomly assigned to either the experimental group or the control group. Experimental rats received an intracerebroventricular (i.c.v.) injection of 6-OHDA (300 µg in 10µl of vehicle). Control rats received an i.c.v. injection of vehicle (10µl of 0.3% ascorbic acid dissolved in saline). After surgery, rats were returned to their home cages. For the first two weeks after surgery rats were placed in constant darkness (24hr D cycle).

For the third and fourth weeks after surgery rats were re-entrained to a normal 12:12hr LD cycle. At the end of the fourth week, rats from each group were randomly assigned to be perfused at either zeitgeber time 1 (ZT1) or ZT14 (in a 12hr:12hr LD cycle, ZT0 is when lights go on and ZT12 is when lights go off). Each experiment consisted of 12 rats and the procedure was repeated 4 times for a total of 48 treated rats in the present study.

Surgery and Injections

Thirty minutes prior to anaesthesia, rats were injected intra-peritoneally with 1.0ml/kg of Desipramine (25mg/ml) in order to protect noradrenergic neurons from 6-OHDA induced damage. Rats were then anaesthetized with a mixture of Ketamine (100mg/ml) and Xylazine (20mg/ml) by i.p injection of 0.8ml/kg of the mixture. Anaesthetized rats were mounted on a stereotaxic frame (Stoelting, Wood Dale, IL). A small incision was made in the scalp, and a small hole was drilled at the appropriate coordinates from bregma for i.c.v. drug administration (anterior-posterior [AP] -0.84mm, medial-lateral [ML] 0.0mm, dorsal-ventral [DV] -7.1, from dura). A Hamilton 25 μ l syringe was loaded with 10 μ l of 6-OHDA or vehicle, and using the stereotaxic, a needle tip was lowered into the appropriate location. Drug or vehicle was infused at a rate of 1 μ l/minute for 10 minutes. The needle was then retracted to DV -6.1 from dura and left there for two minutes to ensure proper absorption. The needle was then fully retracted and the hole in the skull was filled with sterile bone wax. A layer of sticky-wax was applied to seal the hole. Hibitane (Bioglan), an antifungal and antiseptic cream, was applied directly into the wound and the scalp was then sutured. Rats received an intramuscular injection of Procillin (MTC Bimeda, Cambridge, ON, 1.5ml per leg, 3ml

total), and a subcutaneous injection of saline or lactated ringer (4ml total). Rats were kept warm under a lamp until they revived and were then transported back to their home cages.

Perfusions and Tissue Preparation

Rats were deeply anesthetized with an i.p. injection of sodium pentobarbital (100 mg/kg, Somnotol, MTC Bimeda). They were then perfused intracardially with cold saline (0.9% NaCl, 300mL) and finally with cold paraformaldehyde (4% in a 1M phosphate buffer, pH 7.3, 300mL). Brains were kept in paraformaldehyde for 24 hours. Brains were then sliced into 50µm thick coronal slices using a vibratome (Vibratome, St-Louis, MO). Brain slices were then rinsed in TBS (3x10minutes) to remove any residual paraformaldehyde before being placed in Watson's Cryoprotectant for storage at -20°C.

Immunohistochemistry

PER2

Brain sections were transferred from Watson's Cryoprotectant to a cold 0.9% Trizma buffered saline (TBS; pH 7.6) rinse (6x10minutes). Using a fine-tipped brush, sections were transferred into the quenching solution (9 parts TBS to 1 part H₂O₂) and left for 30minutes at room temperature before being transferred to a TBS rinse (3x10minutes). Sections were then transferred into the pre-block solution (0.3 % Triton X in TBS and 5.0 % normal goat serum) for 1 hr at 4 °C. Following the pre-block, sections were transferred to the primary solution (goat polyclonal antibody raised against PER2 (Santa Cruz Biotechnology, Inc., Santa Cruz, CA) diluted to 1:4000 in Triton-TBS and 3% normal goat serum (NGS)) and left for 48hours at 4°C on a rotator. Sections were

then transferred to a cold TBS rinse (3x10minutes) and subsequently to the secondary solution (biotinylated anti-rabbit IgG made in goat (Vector Laboratories, Burlington, ON) diluted 1:200 in Triton-TBS and 3 % NGS) and left for 1 hr at 4°C on a rotator.

Following the secondary solution, sections were transferred to a cold TBS rinse (3x10minutes) and then into the ABC solution (avidin-biotin-peroxidase complex, Vectastain Elite ABC Kit, Vector Laboratories) and left for 2hrs at 4°C on a rotator.

Following the ABC phase, sections were transferred to a cold TBS rinse (3x10minutes) followed by a cold 50 mM Tris-HCL rinse (1x10minutes). Sections were then placed in a diaminobenzidine (DAB) solution (0.05 % diaminobenzidine in Tris-HCL) for 10minutes at room temperature, and then transferred to a Nickel Chloride (NiCl₂) solution (0.05% DAB, 0.01 % H₂O₂, and 8 % NiCl₂), for 10 minutes at room temperature. Finally, the sections were transferred to a TBS rinse (3x10minutes) and mounted onto gel-coated slides on the following day. Slices were allowed to dry onto the slides and were then dehydrated by alcohol baths of progressively higher alcohol content. Slides were then transferred to a Citrisolv (Fischer Scientific, Houston, TX) bath for at least 30 minutes to remove any remaining impurities and subsequently coverslipped with Permount (Fischer Scientific).

Tyrosine Hydroxylase

Brain sections were transferred from Watson's Cryoprotectant to a cold TBS rinse (6x10minutes). Using a fine-tipped brush, sections were transferred into the primary solution (mouse monoclonal antibody raised against TH (Chemicon International, Temecula, CA) diluted to 1:10,000 in Triton-TBS and 5% Normal Horse Serum (NHS))

and left for 48 hours at 4°C on a rotator. Sections were then transferred to a cold TBS rinse (3x10 minutes) and subsequently to the secondary solution (biotinylated anti-mouse IgG, rat absorbed, produced in horse (Vector Laboratories, Burlington, ON) diluted to 1:33 in Triton-TBS and 5 % NHS) and left for 1 hr at 4°C on a rotator. Following the secondary solution, sections were transferred to a cold TBS rinse (3x10 minutes) and then into the ABC solution (avidin-biotin-peroxidase complex, Vectastain Elite ABC Kit, Vector Laboratories) and left for 2 hrs at 4°C on a rotator. Following the ABC phase, sections were transferred to a cold TBS rinse (3x10 minutes) followed by a cold 50 mM Tris-HCL rinse (1x10 minutes). Sections were then placed in a diaminobenzidine (DAB) solution (0.05 % diaminobenzidine in Tris-HCL) for 10 minutes at room temperature, and then transferred to a hydrogen peroxide (H₂O₂) solution (0.05% DAB and 0.01 % H₂O₂), for 10 minutes at room temperature. Finally, the sections were transferred to a TBS rinse (3x10 minutes) and mounted onto gel-coated slides on the following day. Slices were allowed to dry onto the slides and were then dehydrated by alcohol baths of progressively higher alcohol content. Slides were then transferred to a Citrisolv (Fischer Scientific, Houston, TX) bath for at least 30 minutes to remove any remaining impurities and subsequently coverslipped with Permount (Fischer Scientific).

Data Analysis

Behavior

Actograms generated by the VitalView system, and subsequently plotted on Circadia Software, were visually analyzed in order to determine rats entrainment to the 12:12 LD cycle, as well as to determine overall and, more specifically, post-surgery

locomotor activity. Also, rats were visually observed for a few minutes each day for 4 consecutive days post-surgery and subsequently, every other day, and any abnormal behaviour was noted.

A repeated measures t-test was used to analyze pre- vs. post- surgery activity levels (i.e., number of wheel revolutions per 10 minute time bin) for both sham and 6-OHDA groups.

Brain

Seven brain areas (SCN, BNSTov, BLA, CEA, DG, PV, and striatum) were captured under a light microscope (Leitz Laborlux S) using a video camera (Sony XC-77) connected to a frame grabber (Scion LG-3) with image software (NIH v1.63). Bilateral images of each brain area were photographed within a 400x400 μ m template at 20x magnification. Immuoreactive cells were counted using Image SXM software (v1.79). The average of the 5 sections containing the greatest number of stained nuclei was used for each animal.

The areas of interest were examined using a 2-way analysis of variance (ANOVA) with condition (6-OHDA/Sham) and zeitgeber time (ZT1/ZT14) as independent variables. For any analyses that yielded a significant interaction effect, t-tests were conducted in order to determine where the differences between the factors lay.

The striatum was further analyzed using a mixed design ANOVA with extent of lesion (strong/weak) as the within subjects factor and zeitgeber time (ZT1/ZT14) as the between subjects factor. The alpha level was set at .05 for all analyses.

RESULTS

Behavior

Entrainment

All rats were entrained to the 12-hr:12-hr LD schedule within the two weeks prior to surgery. Rats were considered entrained if they used the running wheels mostly during the dark phase of the cycle and if activity onset coincided with the onset of the dark phase of the cycle (see figures 1 and 2, from days 0-15).

Post surgery

Approximately 1/3 of all 6-OHDA treated rats died within the first few days post surgery, whereas only 1/10 of all sham treated rats died during this time.

On average, rats in the sham group took 3 days to recover from surgery, i.e., rats in the sham group resumed activity approximately 3 days post surgery (see figure 1, days 16-19) whereas rats in the 6-OHDA group did not resume activity until approximately 7 days post surgery (see figure 2, days 15-21 and figure 3, days 14-19). Not only did 6-OHDA group rats cease wheel-running in the days post-surgery, but they also ceased grooming themselves as evidenced by dried urine covering the abdominal area and the tail, and by the accumulation of dried porphyrin around the eyes.

Unlike sham group rats that started eating soon after waking up from surgery, all 6-OHDA lesioned rats displayed severe adipsia (absence of drinking) and aphagia (absence of eating) and had to be injected daily with lactated ringer in order to prevent dehydration. Approximately 1/4 of the rats did not resume eating even at 7 days post surgery, lost a significant amount of body mass, and were thus euthanized before the end

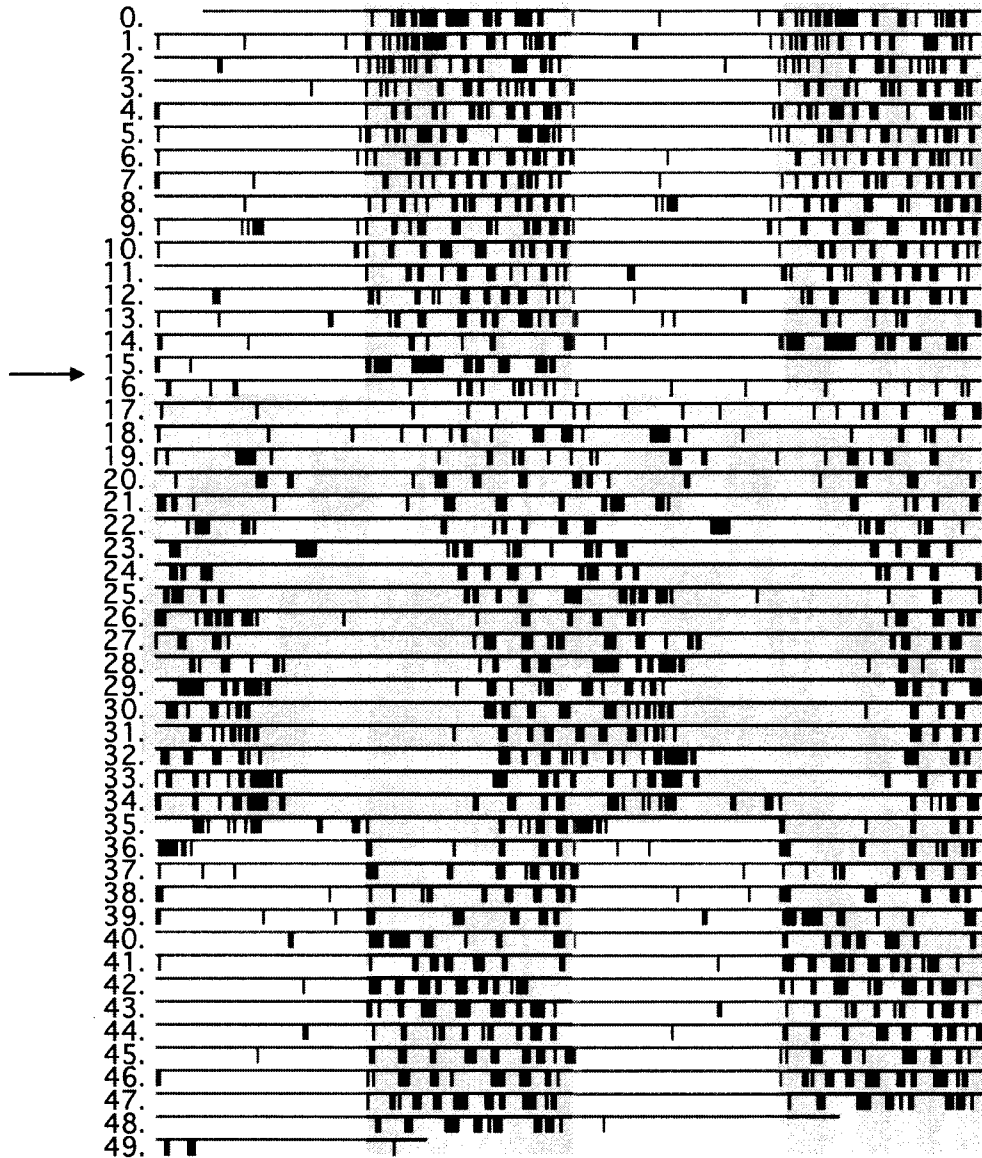


Figure 1. Representative double plotted actogram from a sham rat. The numbers indicate the day, starting with day 0 when rats were first placed in the boxes. Vertical marks indicate periods of activity of at least 10 wheel revolutions/10 min. White background indicates lights on, grey background indicates lights off. Arrow indicates surgery day.

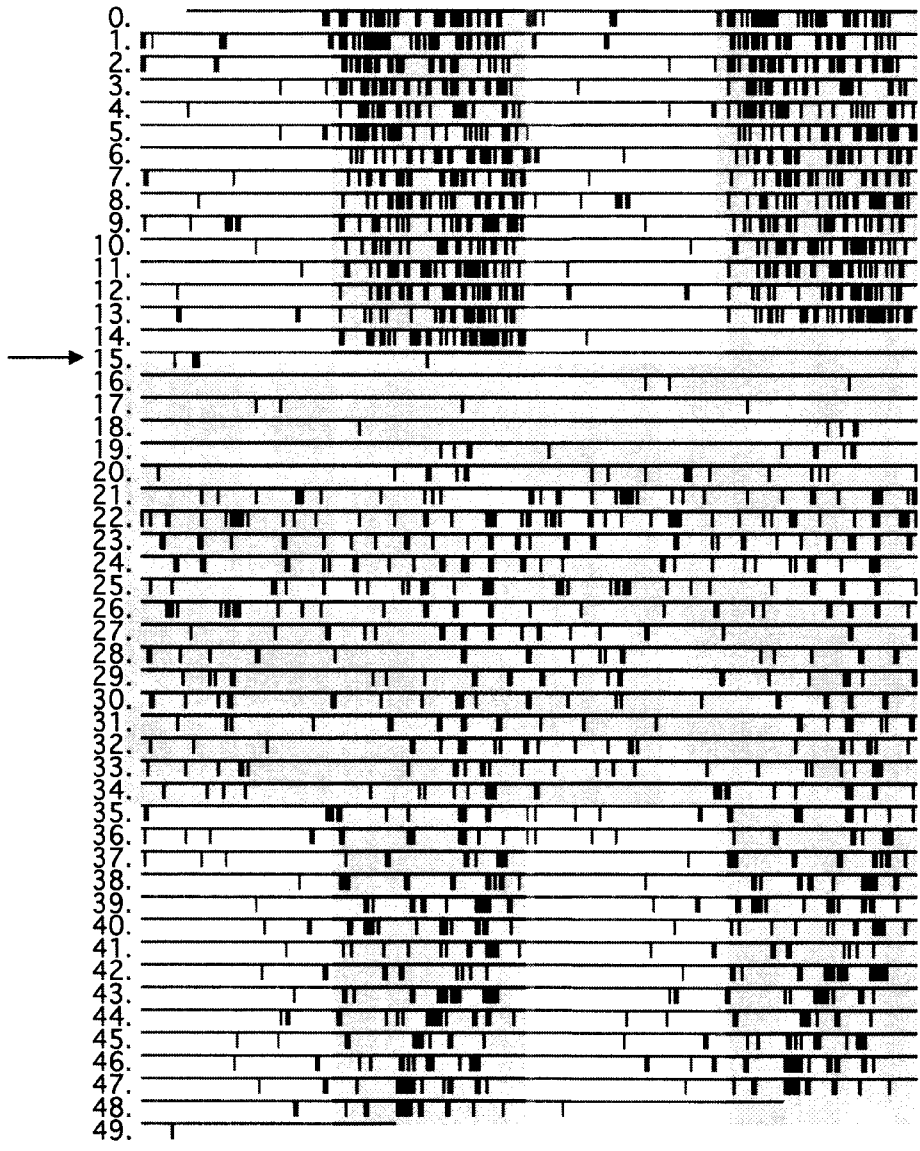


Figure 2. Representative double plotted actogram from a 6-OHDA lesioned rat. The numbers indicate the day, starting with day 0 when rats were first placed in the boxes. Vertical marks indicate periods of activity of at least 10 wheel revolutions/10 min. White background indicates lights on, grey background indicates lights off. Arrow indicates surgery day.

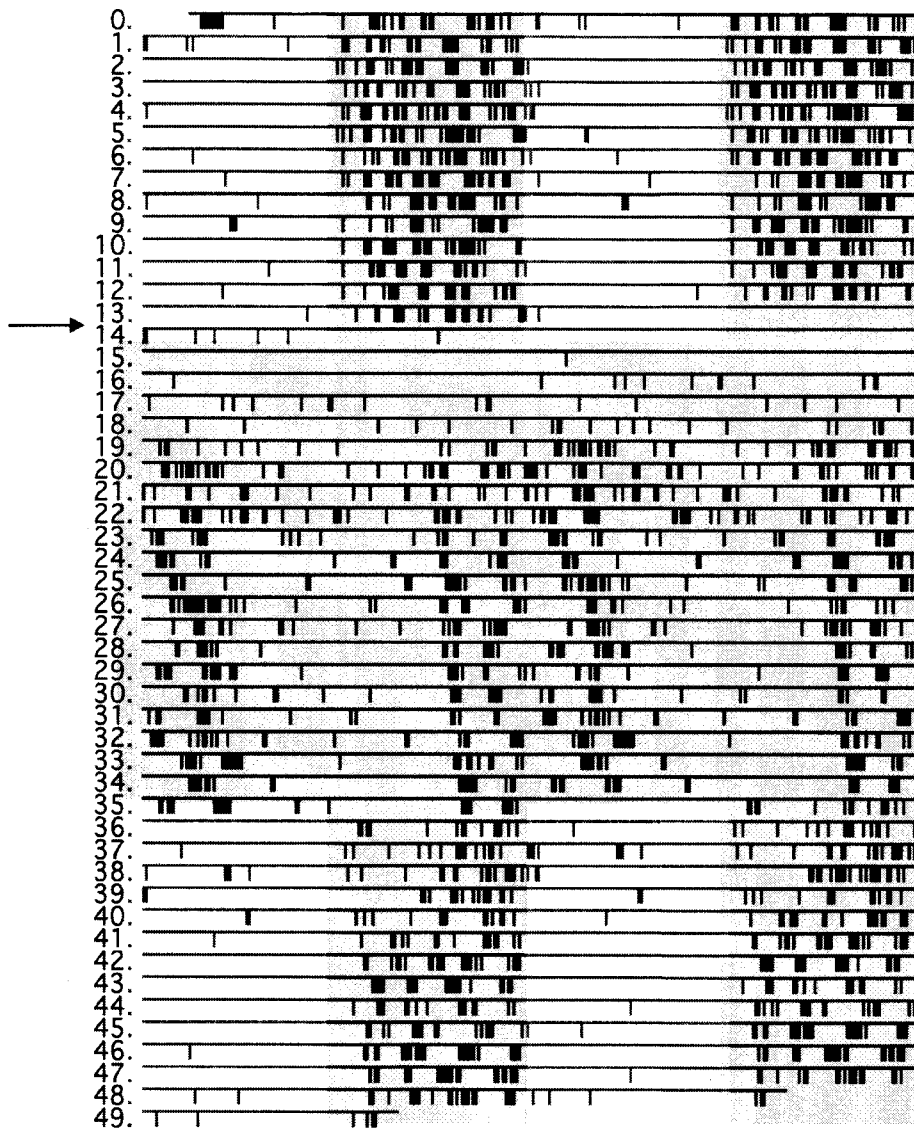


Figure 3. Representative double plotted actogram from a 6-OHDA lesioned rat. The numbers indicate the day, starting with day 0 when rats were first placed in the boxes. Vertical marks indicate periods of activity of at least 10 wheel revolutions/10 min. White background indicates lights on, grey background indicates lights off. Arrow indicates surgery day.

of the experiment. Of the rats that survived, many had bladder infections due to the severe decrease in urination that accompanied the dehydration and were thus treated with penicillin.

All 6-OHDA lesioned rats displayed abnormal behavior to varying degrees. Any attempt to hold one of these rats, or any sudden loud noise, was met with an uncontrolled and uncoordinated flee response that resulted in the rat crashing against the walls and ceiling of the metal cage for up to five seconds and with such force that we feared the behavior could result in injury. However, no rat was injured as a result of this behavior. Most rats, including those that displayed the exaggerated startle response, were mostly akinetic unless startled, handled, or prodded. Most rats also displayed an uncharacteristic hopping behavior in which they would use their hind legs to propel themselves upwards with enough height to escape from the holding cage if the lid was not secured. Immediately upon waking or within the first day of surgery, some rats, after the aforementioned flee response, would assume an arched-back position with the upper body and front paws pressed up against the side of the cage and remain there, immobile, for several hours. All of the rats that displayed this behavior died within the first few days post surgery. A few of the rats also displayed defensive behaviors, i.e., biting, when experimenters tried to retrieve them from their cages. These were abnormal in that the rat would lock its jaw on the experimenter's glove for several minutes and would not release its hold even when lifted or moved.

Constant Darkness

As can be seen in figure 1, sham rats resumed normal activity levels post-surgery (no significant difference in the number of daily wheel revolutions pre- vs. post-surgery,

$t(11) = 1.827, p > .05$). However, as can be seen in figure 2, 6-OHDA rats showed a marked (70%) decrease in activity levels ($t(13) = 4.479, p < .05$).

Sham rats displayed normal free-running rhythms in constant darkness (see figure 1, days 17-34). The diagonal marked by the daily delay of the onset of activity represents the free running rhythm of rats, which in constant darkness is slightly longer than 24 hours. Note that although sham rats are in constant darkness, they exhibit daily cycles of approximately 12 hours of activity followed by approximately 12 hours of rest. In contrast to this, most of the 6-OHDA rats displayed a disorganization of their activity rhythm in the first few days of re-instatement of activity post surgery. As exemplified in figure 2 (days 21-27), figure 3 (days 17-22), and figure 4 (days 17-24) 6-OHDA lesioned rats' wheel-running was not limited to the subjective night (i.e., time of lights off if the 12:12 LD cycle had continued) as seen with sham group rats: activity was also observed during the subjective day. Ten of the thirteen 6-OHDA rats displayed blunted activity rhythms in the first 3-7 days post surgery. Most of these rats resumed normal free-running activity rhythms after these first few days (see figure 3, days 24-34 and figure 4, days 26-34). Three of the thirteen 6-OHDA rats displayed normal free running activity upon commencement of activity post surgery (see figure 5, days 18-34).

Re-entrainment

Both sham and 6-OHDA lesioned rats were able to re-entrain to the 12h:12h LD cycle imposed after the two weeks of constant darkness (see figures 1 and 2). Sham group rats entrained within 2-5 days after the start of the LD cycle and 6-OHDA group rats entrained within 2-10 days after the start of the LD cycle, displaying a larger variability in rate of entrainment.

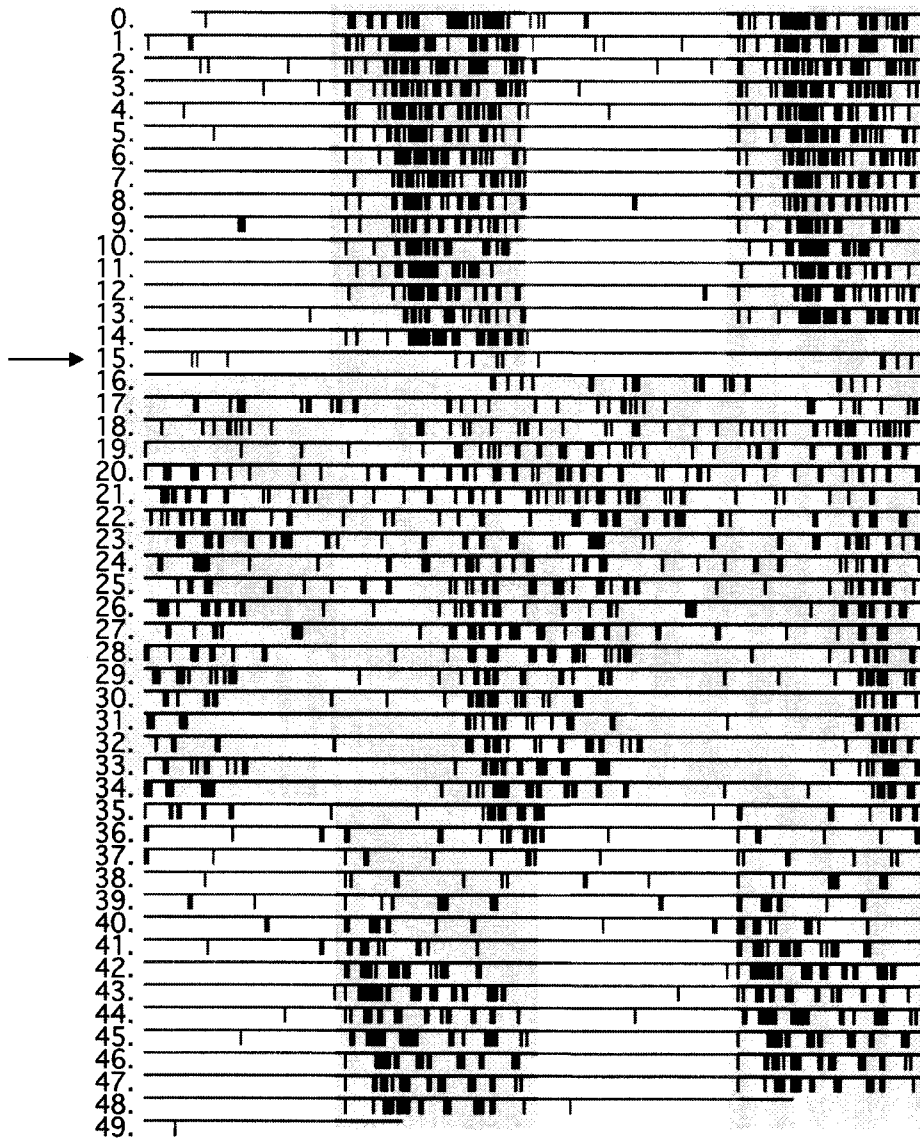


Figure 4. Representative double plotted actogram from a 6-OHDA lesioned rat. The numbers indicate the day, starting with day 0 when rats were first placed in the boxes. Vertical marks indicate periods of activity of at least 10 wheel revolutions/10 min. White background indicates lights on, grey background indicates lights off. Arrow indicates surgery day.

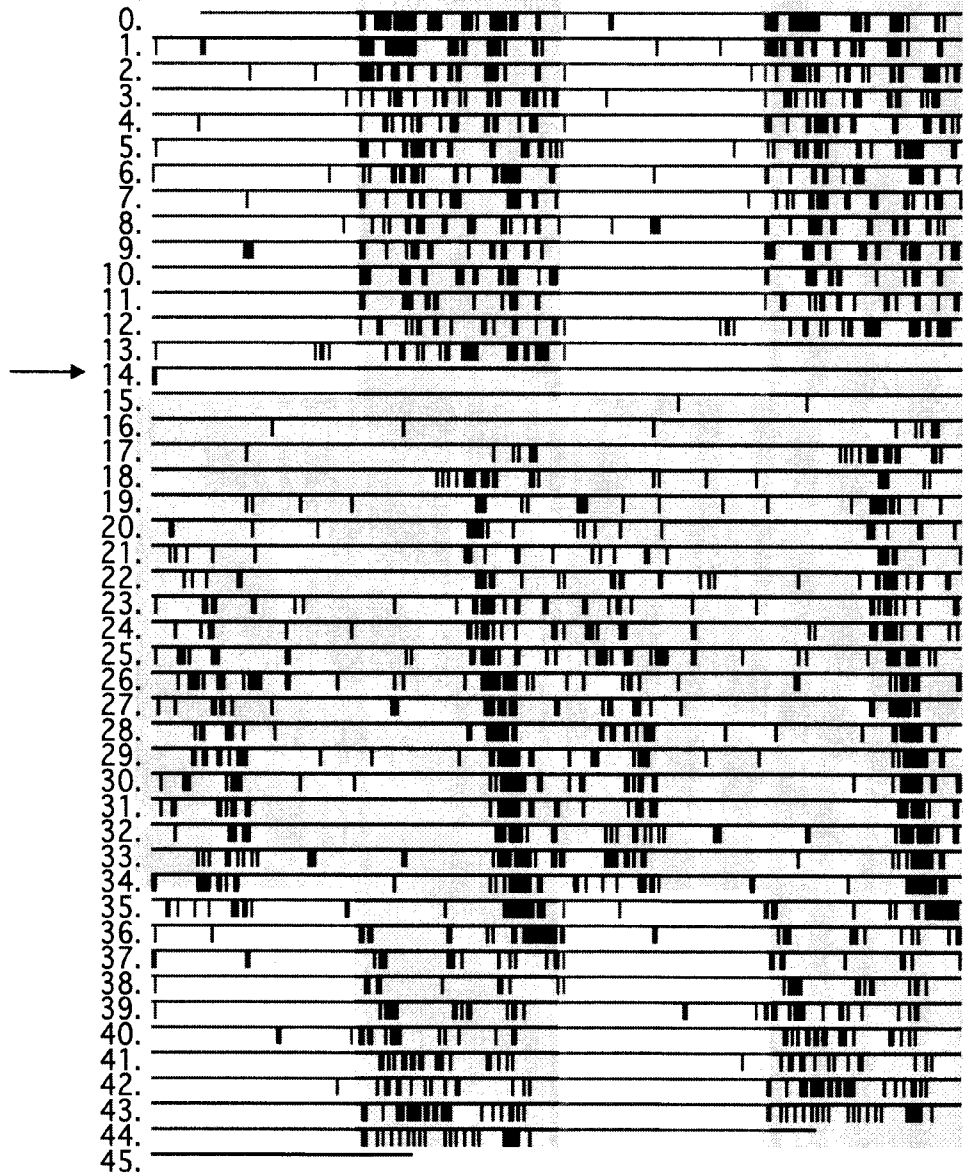


Figure 5. Representative double plotted actogram from a 6-OHDA lesioned rat. The numbers indicate the day, starting with day 0 when rats were first placed in the boxes. Vertical marks indicate periods of activity of at least 10 wheel revolutions/10 min. White background indicates lights on, grey background indicates lights off. Arrow indicates surgery day.

Striatum

TH

One of the goals of injection of 6-OHDA into the third ventricle was to achieve a bilateral depletion of dopamine levels in the striatum, and to that effect we expected 6-OHDA rats to show fewer TH-ir fibers than controls. Indeed, all experimental rats had dramatically less TH-ir fibers than controls. Eight out of seventeen 6-OHDA lesioned rats displayed the same degree of reduction in TH-ir fibers in both right and left hemispheres. However, nine out of seventeen 6-OHDA lesioned rats had uneven lesions with five of these nine displaying less TH-ir fibers in the left hemisphere than in the right hemisphere and four of these nine rats displaying less TH-ir fibers in the right hemisphere than in the left hemisphere.

Figure 6 shows representative photomicrographs of sections stained with TH for a sham rat and a 6-OHDA rat with an even lesion. Unlike tissue from the sham group, which shows dark staining throughout the striatum due to the dense clustering of TH-ir fibres, tissue from the 6-OHDA group is characterized by weak staining throughout the striatum, due to the presence of sparse and isolated axons. While the number of stained axons in sham group tissue is so large that it is not possible to distinguish one axon from another, the apparent lack of stained axons in the 6-OHDA group tissue allows for visualization of individual axons (see figures 6C and 6D). The dramatic decrease in TH-ir fibers in the 6-OHDA group tissue suggests that treatment with 6-OHDA was effective in depleting dopamine levels in the striatum.

Figure 7 shows representative photomicrographs of sections stained with TH for rats with uneven lesions (figure 7B) and for sham rats (figure 7A). As is clear from the

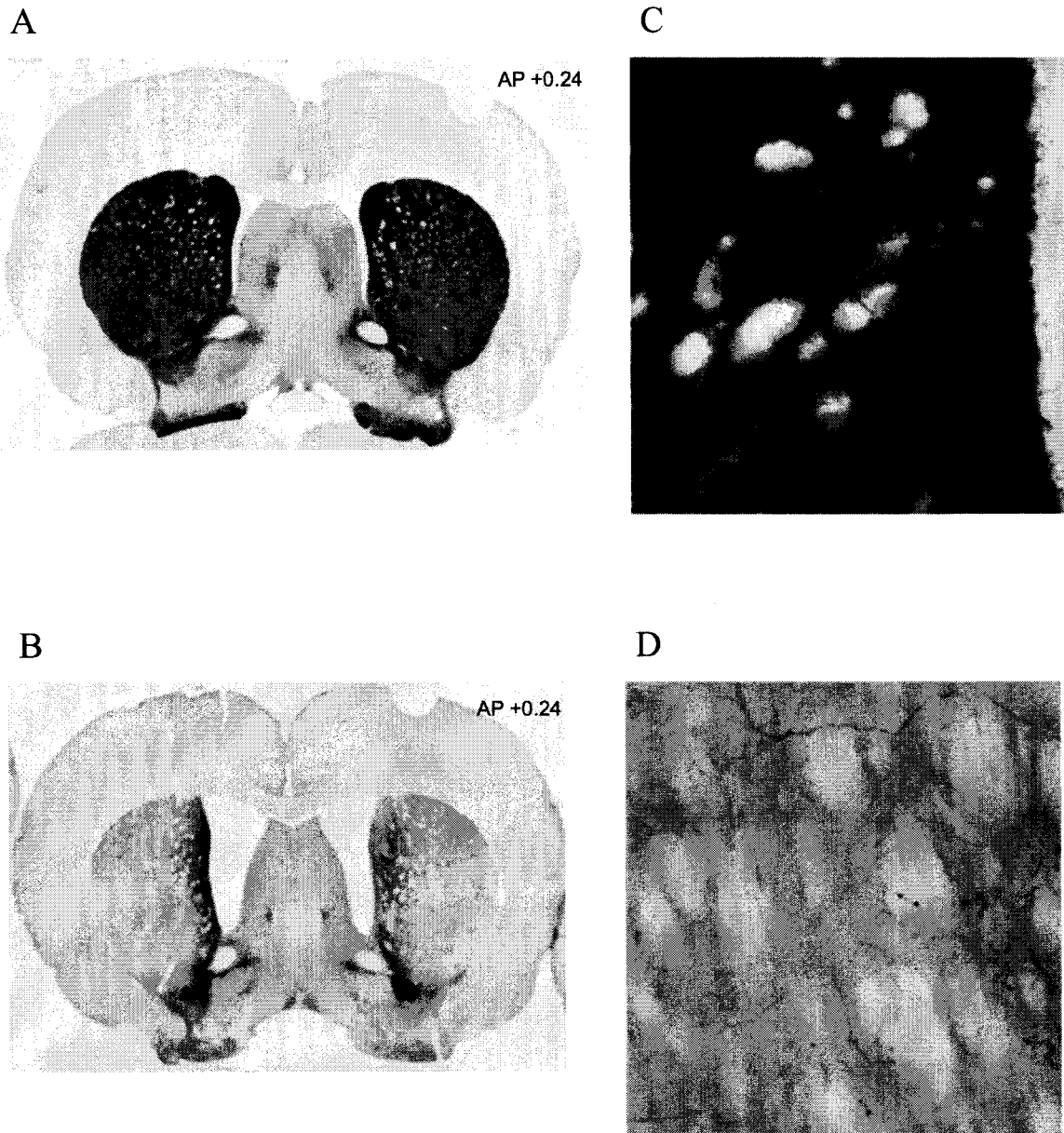


Figure 6. Representative photomicrographs of TH-ir fibers in the striatum at 5x (A,B) and 20x (C,D) magnification of sham (A,C) and 6-OHDA lesioned (B,D) rats perfused 4 weeks after surgery.

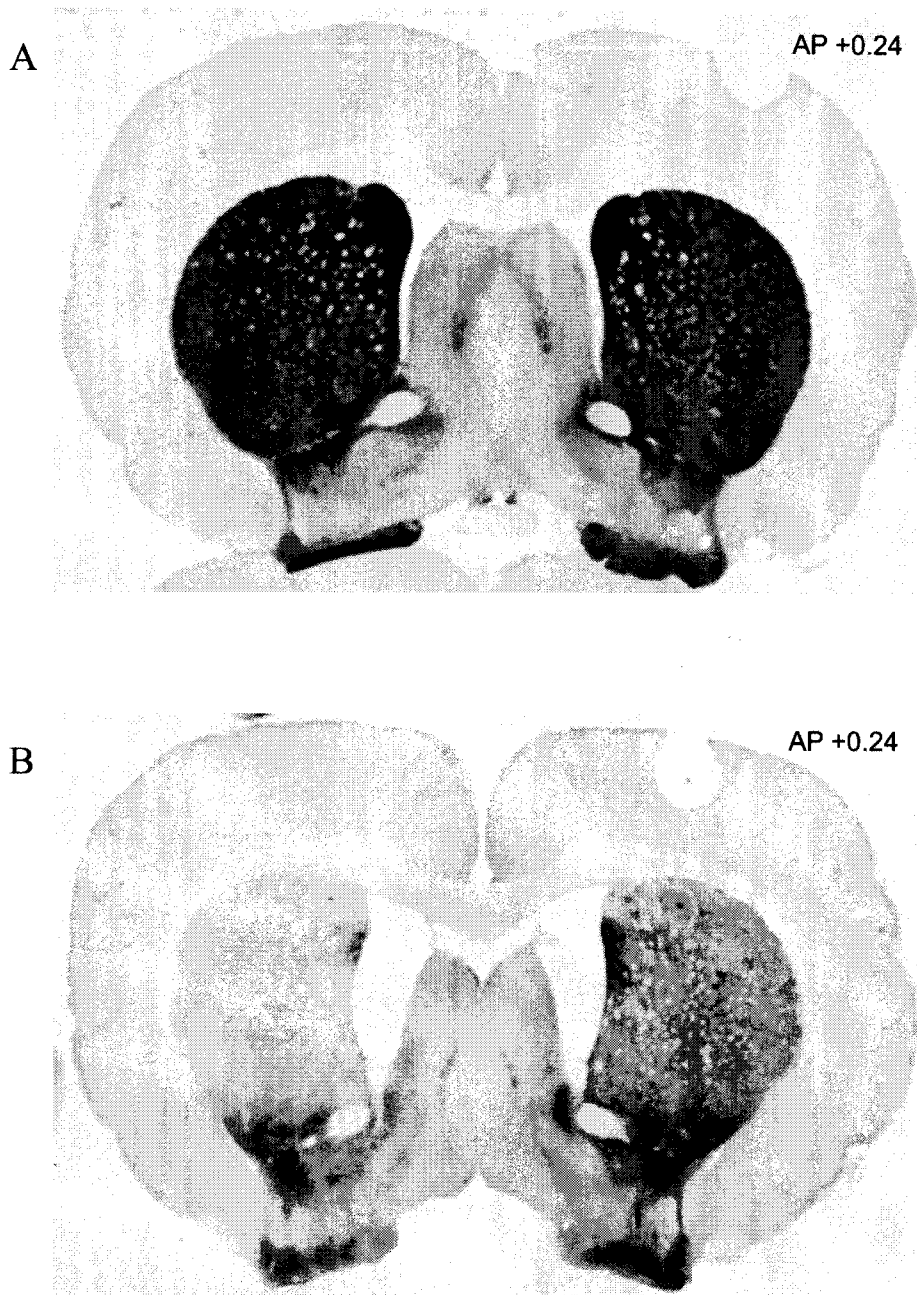


Figure 7. Representative photomicrographs of TH-ir fibers in the striatum of a sham rat (A) and a 6-OHDA rat with an uneven lesion (B) perfused 4 weeks after surgery .

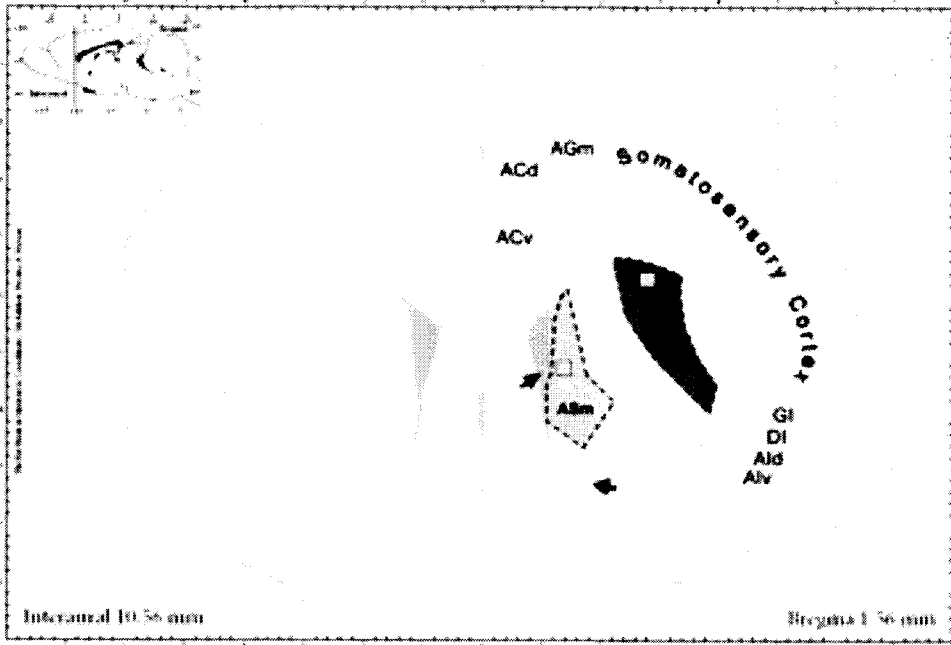
opaqueness of the stain, the right side has more TH-ir fibers than the left side. The side with the greater number of TH-ir fibers, however, still has less TH-ir fibers than the corresponding side of the sham rat.

PER2

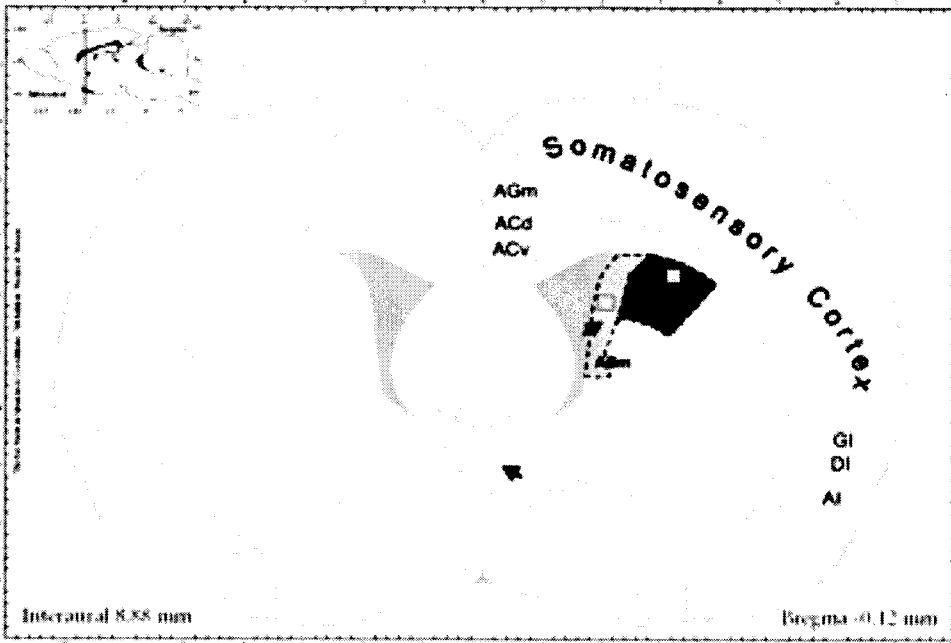
For analysis of PER2 expression in the striatum, we subdivided the striatum into four areas based on anatomical considerations of afferent projections (see figure 8). These areas are: anterior medial (antM), anterior lateral (antL), posterior medial (posM), and posterior lateral (posL). The anterior medial area is the area adjacent to the lateral ventricle at ~5mm (DV) extending from 1.08mm to -0.12mm (AP). The anterior lateral area is the area immediately ventral to the corpus callosum at ~3.5mm (VL) also extending from 1.08mm to -0.12mm (AP). The posterior medial area is adjacent to the lateral ventricle at ~4mm (DV) extending from -0.24 to -1.72mm (AP). The posterior lateral area is immediately ventral to the corpus callosum at ~4.5mm (VL) also extending from -0.24 to -1.72mm (AP).

As more than half of the 6-OHDA lesioned rats displayed uneven lesions of the striatum, one question that arose was whether the extent of the lesion would have an effect on PER2-ir cell counts. We used two analyses in order to answer this question. The first analysis was conducted in order to determine whether there would be a difference in PER2-ir counts between the two hemispheres of rats with uneven lesions. This analysis included only rats with uneven lesions and compared PER2-ir cell counts in the hemisphere with the stronger lesion with the counts in the hemisphere with the weaker lesion. The second analysis was conducted in order to determine whether there would be

A



B



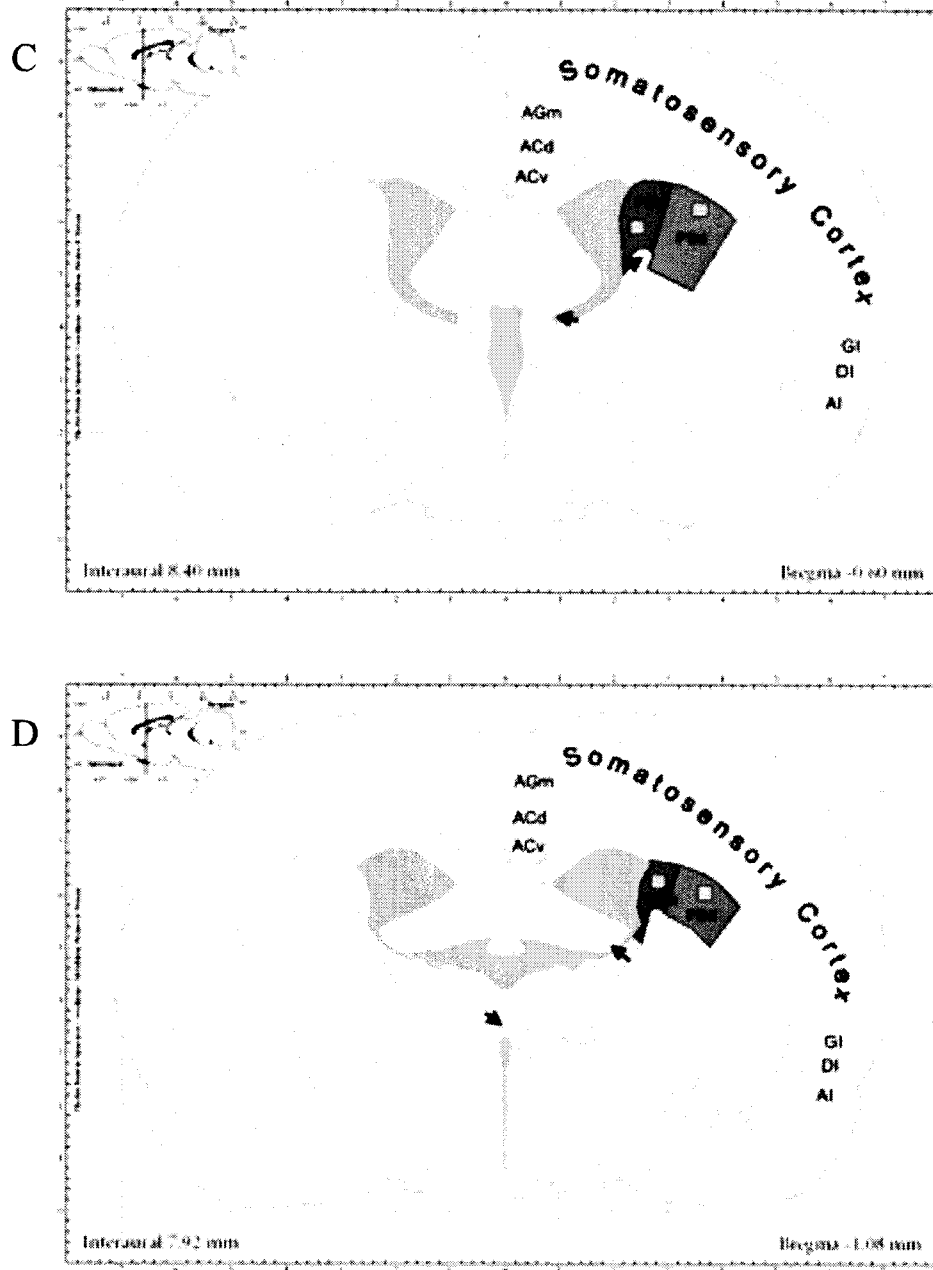


Figure 8. Stereotaxic maps of areas captured in the striatum. Panels A and B depict the anterior striatum and panels C and D depict the posterior striatum. Yellow areas show the anteromedial striatum, red areas show the anterolateral striatum, orange areas show the posteromedial striatum, and green areas show the posterodorsal striatum. Arrows show landmarks used to ensure localization of the area. Small grey boxes represent the target area within which the 400x400mm picture used for the PER2 analysis was taken (figures modified from Paxinos & Watson, 2004).

differences in PER2-ir counts between rats with even lesions and those with uneven lesions. This analyses included both groups of 6-OHDA rats, i.e., those with uneven lesions and those with even lesions, and compared PER2-ir cell counts in the hemisphere with the stronger lesion of the uneven lesion group with the corresponding hemisphere in the even lesion group.

The first analyses was conducted using a mixed design ANOVA with extent of lesion (strong/weak) as the within subjects factor and ZT (ZT1/ZT14) as the between subjects factor. Neither the main effect of lesion ($F(1,7) = 2.467, p > .05$) nor the interaction effect between the factors ($F(1,7) = 1.843, p > .05$) were significant, suggesting that there was no difference between hemispheres in the number of PER2-ir cells even though one hemisphere had a stronger lesion than the other.

The second analyses revealed no significant effect of inequality (rats with even lesions/rats with uneven lesions, $F(1,13) = 2.287, p > .05$) and no significant effect of ZT (to be discussed in the next section, $F(1,13) = 2.410, p > .05$) or of the interaction between the two variables ($F(1,13) = .003, p > .05$). These results suggest that both sub groups of 6-OHDA lesioned rats, i.e., those with an even lesion and those with an uneven lesion display similar PER2-ir cell counts despite the difference in the quality of the lesion.

As the difference in PER2-ir counts between rats with a varying quality of lesion was negligible, rats with even and uneven lesions were grouped together as '6-OHDA' for the main analyses of the striatum. Also, as the difference in PER2-ir counts between the two hemispheres of unevenly lesioned 6-OHDA rats was negligible, counts for the

left and right hemispheres of each region of the striatum were averaged together and this final score was used for the main analyses of each region.

Figure 9 shows the mean counts of PER2-ir cells in the four regions of the striatum. Analyses of the anterior medial striatum revealed a significant interaction effect between condition and ZT ($F(1,24) = 50.946, p < .05$). This was also observed in the anterior lateral ($F(1,24) = 25.440, p < .05$), posterior medial ($F(1,24) = 45.688, p < .05$), and posterior lateral ($F(1,24) = 26.344, p < .05$) striatum.

Anterior Striatum

As expected, the sham group showed higher PER2-ir cell counts at ZT1 than at ZT14 (antM: $t(10) = 9.815, p < .05$, antL: $t(5.126) = 5.530, p < .05$). The 6-OHDA group also had higher counts at ZT1 than at ZT14 (antM: $t(14) = 2.282, p < .05$, antL: $t(14) = 2.720, p < .05$). Differences between the two groups were found when both time points were analyzed separately. At ZT1 the 6-OHDA group had significantly less PER2-ir cells than the sham group (antM: $t(11) = -7.992, p < .05$, antL: $t(5.896) = -4.858, p < .05$). At ZT14, however, both groups had similar numbers of PER2-ir cells (antM: $t(13) = -.990, p > .05$, antL: $t(13) = -1.724, p > .05$).

Posterior Striatum

As expected, the sham group showed higher PER2-ir cell counts at ZT1 than at ZT14 (posM: $t(10) = 9.719, p < .05$, posL: $t(5.252) = 5.379, p < .05$). The 6-OHDA group, however, had similar PER2-ir cell counts at ZT1 and ZT14 (posM: $t(14) = 1.941,$

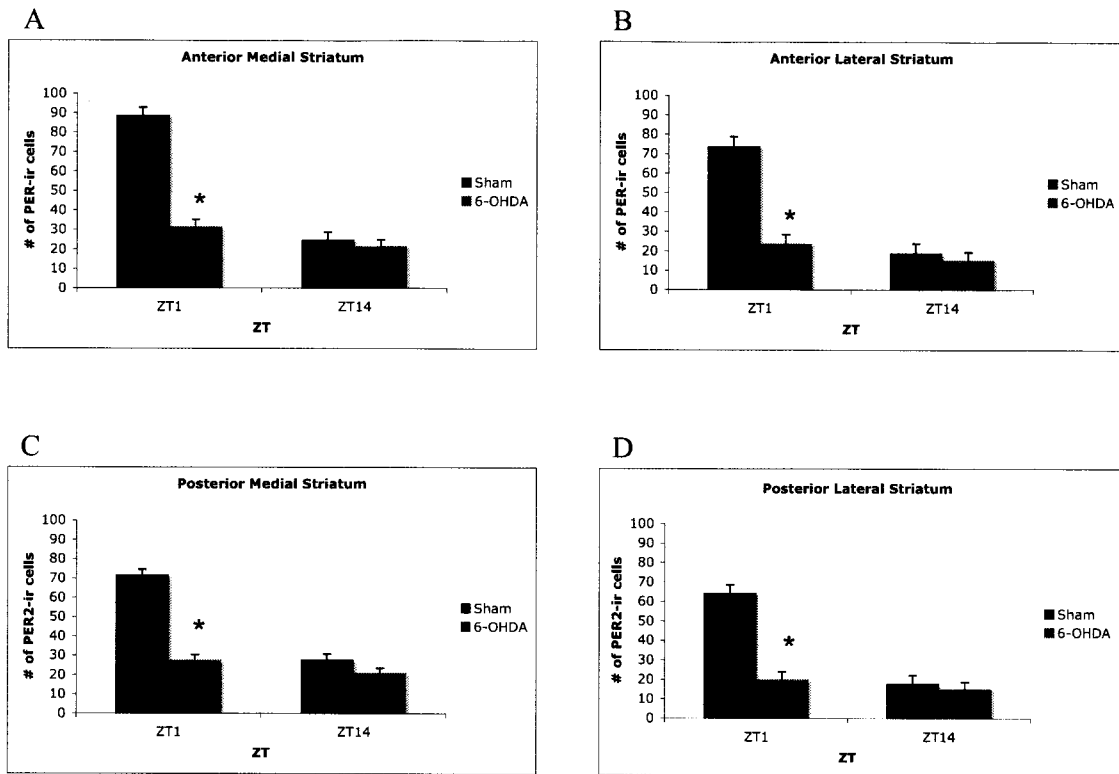


Figure 9. Mean number (\pm SEM) of PER2-ir cells in the anterior medial (A), anterior lateral (B), posterior medial (C), and posterior lateral (D) striatum for sham and 6-OHDA lesioned rats perfused 4 weeks after surgery. $n = 6$ per time point for the sham group. $n = 7$ at ZT1 and $n = 9$ at ZT14 for the 6-OHDA group.

$p > .05$, posL: $t(14) = 1.714$, $p > .05$). At ZT1 the 6-OHDA group had significantly less PER2-ir cells than the sham group (posM: $t(11) = -9.529$, $p < .05$, posL: $t(5.944) = -4.979$, $p < .05$). At ZT14, however, both groups had similar numbers of PER2-ir cells (posM: $t(13) = -2.132$, $p > .05$, posL: $t(13) = -1.335$, $p > .05$).

SCN

PER2

Figure 10 shows representative photomicrographs of the SCN for both the 6-OHDA and sham groups at both time points examined. Figure 11A shows the mean counts of PER2 immunoreactive (PER2-ir) cells for both the 6-OHDA and sham treated groups. As expected, there were significantly more PER2-ir cells at ZT14 than at ZT1 (significant main effect of ZT, $F(1,21) = 145.351$, $p < .05$). However, there was no difference in the number of PER2-ir cells in the SCN of 6-OHDA treated rats when compared to sham rats (non-significant main effect of condition, $F(1,21) = .409$, $p > .05$).

BNSTov

PER2

Figure 11B shows the mean counts of PER2-ir cells in the BNSTov for both the 6-OHDA and sham groups. Analyses of the data revealed a significant interaction effect (condition x ZT, $F(1,24) = 21.87$, $p < .05$). Further analyses revealed that, as expected, the sham group had a greater number of PER2-ir cells at ZT14 than at ZT1 ($t(6.27) = -9.428$, $p < .05$). Also, as reflected in the representative photomicrographs of the BNSTov (figure 12), at ZT1 there was no difference in the number of PER2-ir cells between the

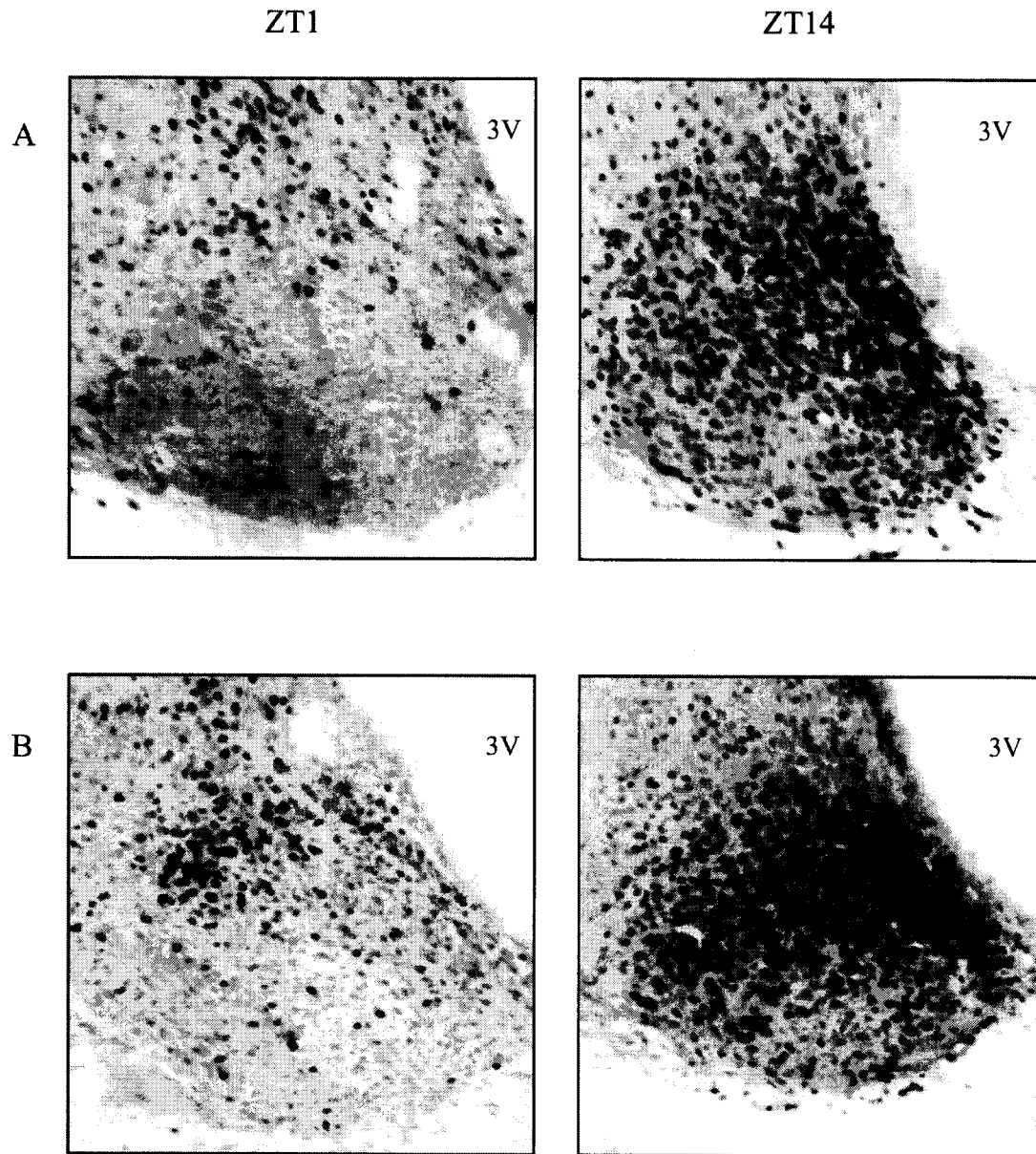


Figure 10. Representative photomicrographs at 10x magnification of PER2-ir cells in the SCN of a sham (A, top panels) and a 6-OHDA lesioned (B, bottom panels) rat at ZT1 and ZT14. 3V = third ventricle.

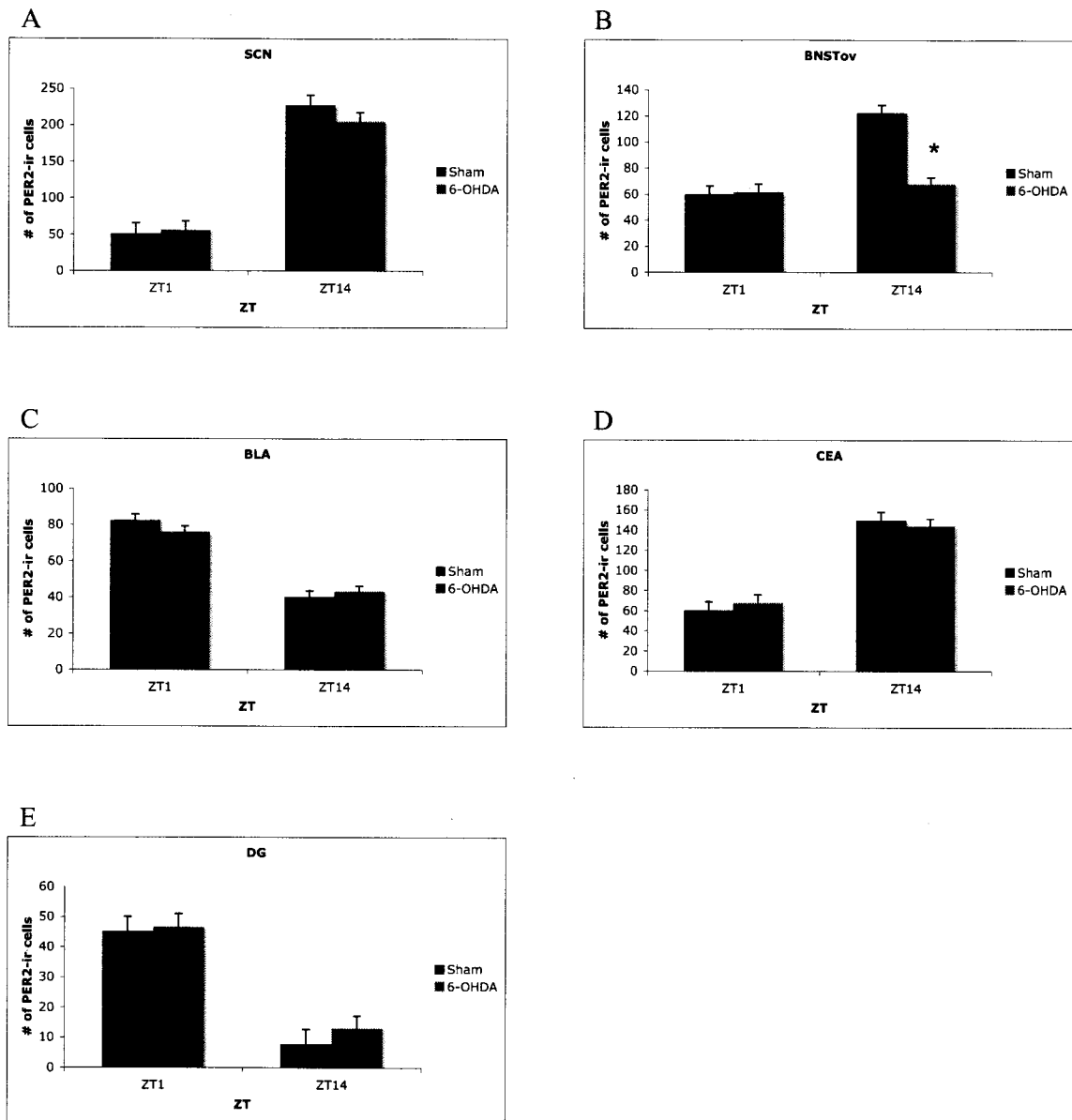


Figure 11. Mean number (\pm SEM) of PER2-ir cells in the SCN (A), BNSTov (B), BLA (C), CEA (D), and DG (E) of sham and 6-OHDA group rats perfused 4 weeks after surgery. $n = 6$ for both time points for the sham group. $n = 7$ at ZT1 and $n = 9$ at ZT14 for the 6-OHDA group.

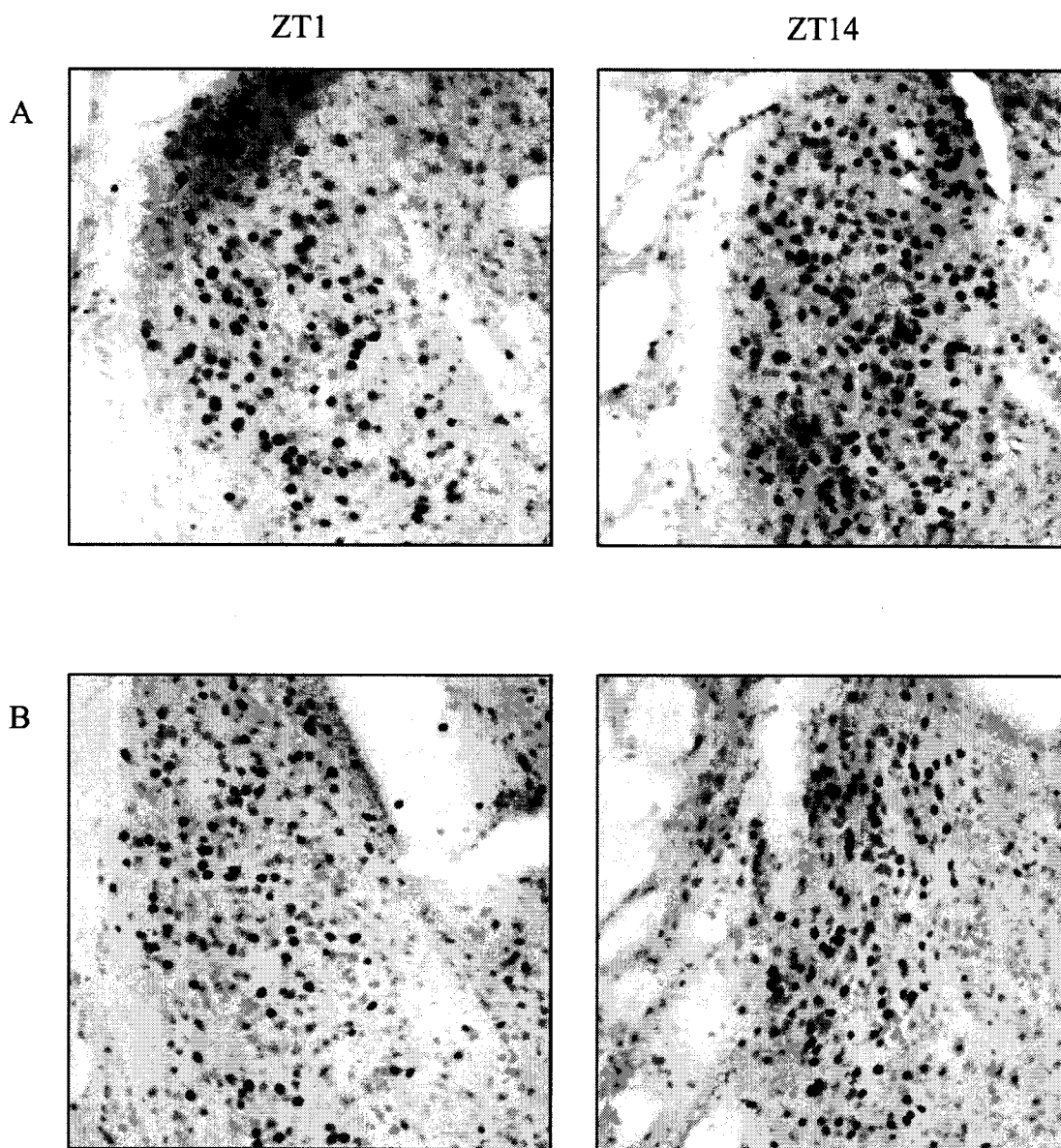


Figure 12. Representative photomicrographs at 10x magnification of PER2-ir cells in the BNSTov of a sham (A, top panels) and a 6-OHDA lesioned rat (B, bottom panels) perfused 4 weeks after surgery at ZT1 and ZT14.

two groups ($t(11) = .459, p > .05$), however, at ZT14 the 6-OHDA group had a significantly lower PER2-ir cell count than the sham group ($t(13) = -5.069, p < .05$) suggesting that the i.c.v 6-OHDA lesion blunted the peak of PER2 expression in the striatum.

TH

Figure 13 shows representative photomicrographs of TH-ir fibers in the BNSTov for a sham rat and a 6-OHDA lesioned rat. There is a clear reduction in the density of TH-ir fibers in the BNSTov of rats that received i.c.v. 6-OHDA compared to those that received a vehicle injection.

CEA

PER2

Figure 11D shows the mean counts of PER2-ir cells in the CEA for both the 6-OHDA and sham groups. As expected there was a greater number of PER2-ir cells at ZT14 than at ZT1 ($F(1,24) = 99.666, p < .05$). Analyses of the data revealed no differences in number of PER2-ir cells in the CEA of 6-OHDA rats when compared to sham rats ($F(1,24) = .014, p > .05$).

TH

Figure 14 shows representative photomicrographs of TH-ir fibers in the CEA of a sham rat and a 6-OHDA rat. There is a clear reduction in the density of TH-ir fibers in the CEA of rats that received i.c.v. 6-OHDA compared to those that received a vehicle injection.

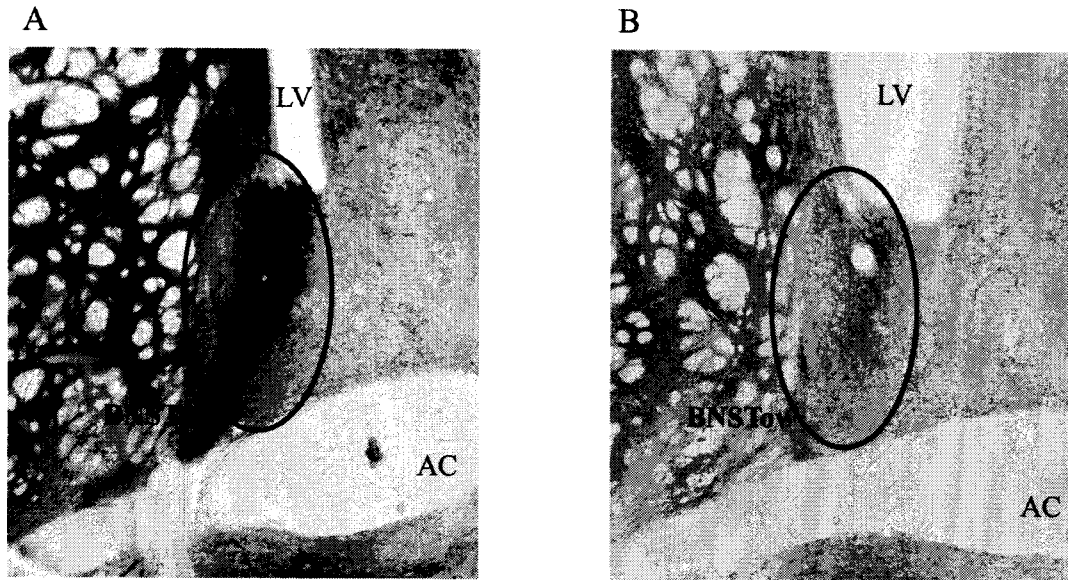


Figure 13. Representative photomicrographs at 5x magnification of TH-ir fibers in the BNSTov (circled) of a sham rat (A) and a 6-OHDA lesioned rat (B) perfused 4 weeks after surgery. LV = lateral ventricle, AC = anterior commissure.

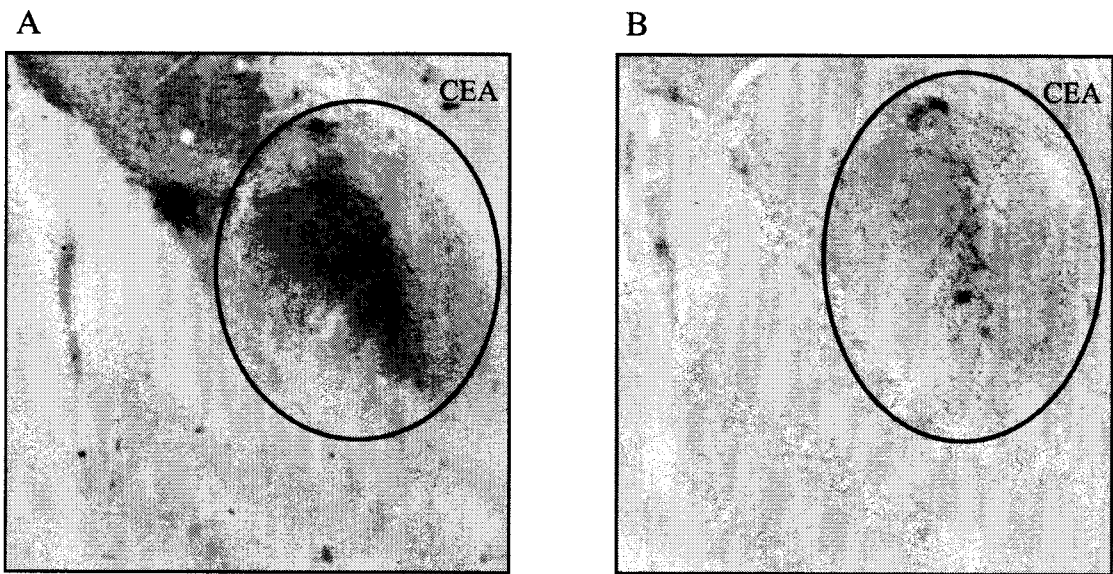


Figure 14. Representative photomicrographs at 10x magnification of TH-ir fibers in the CEA (black circle) of a sham rat (A) and a 6-OHDA lesioned rat (B) perfused 4 weeks post surgery.

BLA

PER2

Figure 11C shows the mean counts of PER2-ir cells in the BLA for both the 6-OHDA and sham groups. As expected, there was a greater number of PER2-ir cells at ZT1 than at ZT14 ($F(1,24) = 134.495, p < .05$). Analyses of the data revealed no differences in number of PER2-ir cells in the BLA of 6-OHDA rats when compared to sham controls ($F(1,24) = .264, p > .05$).

TH

No differences were noted in fiber density of TH-ir fibers between 6-OHDA treated and sham treated rats.

DG

PER2

Figure 11D shows the mean counts of PER2-ir cells in the DG for both the 6-OHDA and sham groups. As expected, there is a greater number of PER2-ir cells at ZT1 than at ZT14 ($F(1,24) = 99.666, p < .05$). Analyses of the data revealed no differences in number of PER2-ir cells in the DG of 6-OHDA rats when compared to sham controls ($F(1,24) = .537, p > .05$).

Periventricular Nucleus

PER2

Figure 15A shows the mean counts of PER2-ir cells in the periventricular nucleus for both the 6-OHDA and sham groups at the two time points examined. Analyses

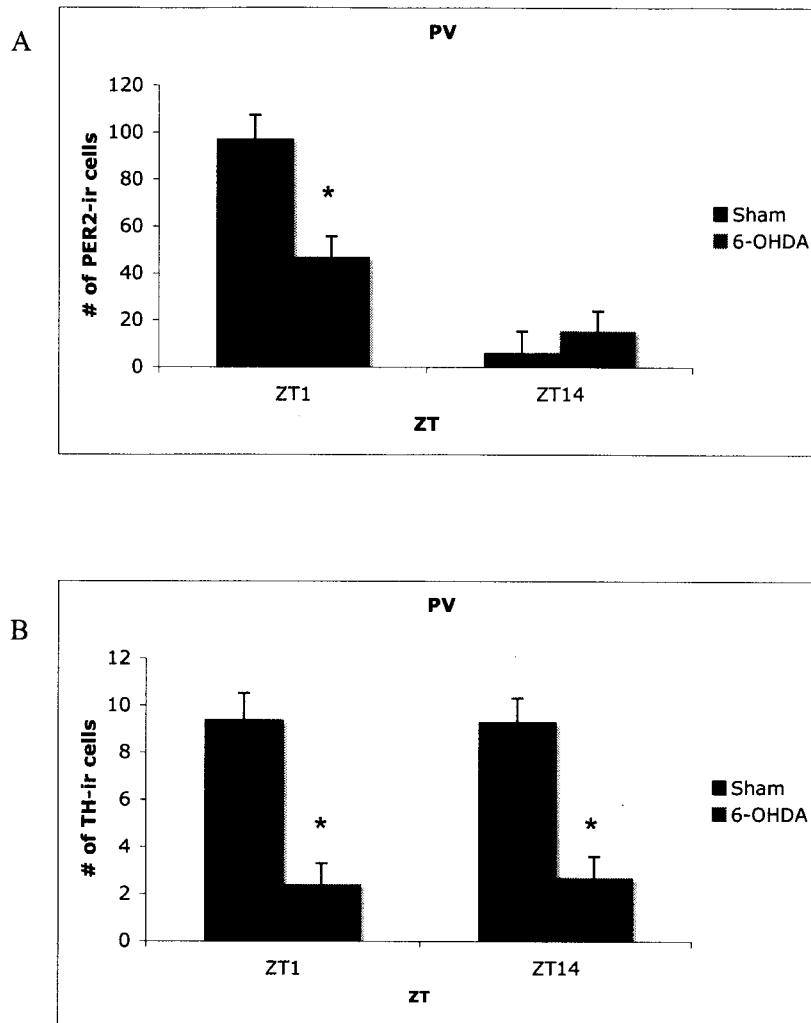


Figure 15. Mean number (\pm SEM) of PER2-ir cells (A) and TH-ir cells (B) in the periventricular nucleus of sham and 6-OHDA group rats perfused 4 weeks after surgery. $n = 6$ for both time points for the sham group. $n = 7$ at ZT1 and $n = 9$ at ZT14 for the 6-OHDA group.

revealed a significant interaction between condition and ZT ($F(1,21) = 10.558, p < .05$). Further analyses showed that for sham rats PER2-ir cell counts were higher at ZT1 than at ZT14 ($t(4.096) = 6.778, p < .05$). 6-OHDA rats also showed this pattern ($t(12) = 2.407, p < .05$); however, at ZT1 the 6-OHDA group had significantly fewer PER2-ir cells in the PV than the sham group ($t(10) = -2.880, p < .05$). At ZT14 there was no difference in PER2-ir cell counts between the groups (see also figure 16). These results suggest that both treatment groups had significantly different numbers of PER2-ir cells at ZT1 compared to ZT14, however, treatment with 6-OHDA blunted the peak of PER2 expression.

TH

Figure 15B shows the mean counts of TH-ir cells in the PV for both the 6-OHDA and sham groups at the two time points examined. Analyses revealed a significant main effect of condition; the 6-OHDA group had lower counts of TH-ir cells when compared to the sham group ($F(1,21) = 49.680, p < .05$). Neither ZT nor the interaction between condition and ZT achieved significance. The observation of significantly lower counts of TH-ir cells across time points for the 6-OHDA group corroborates the efficacy of the treatment in this area (see figure 17).

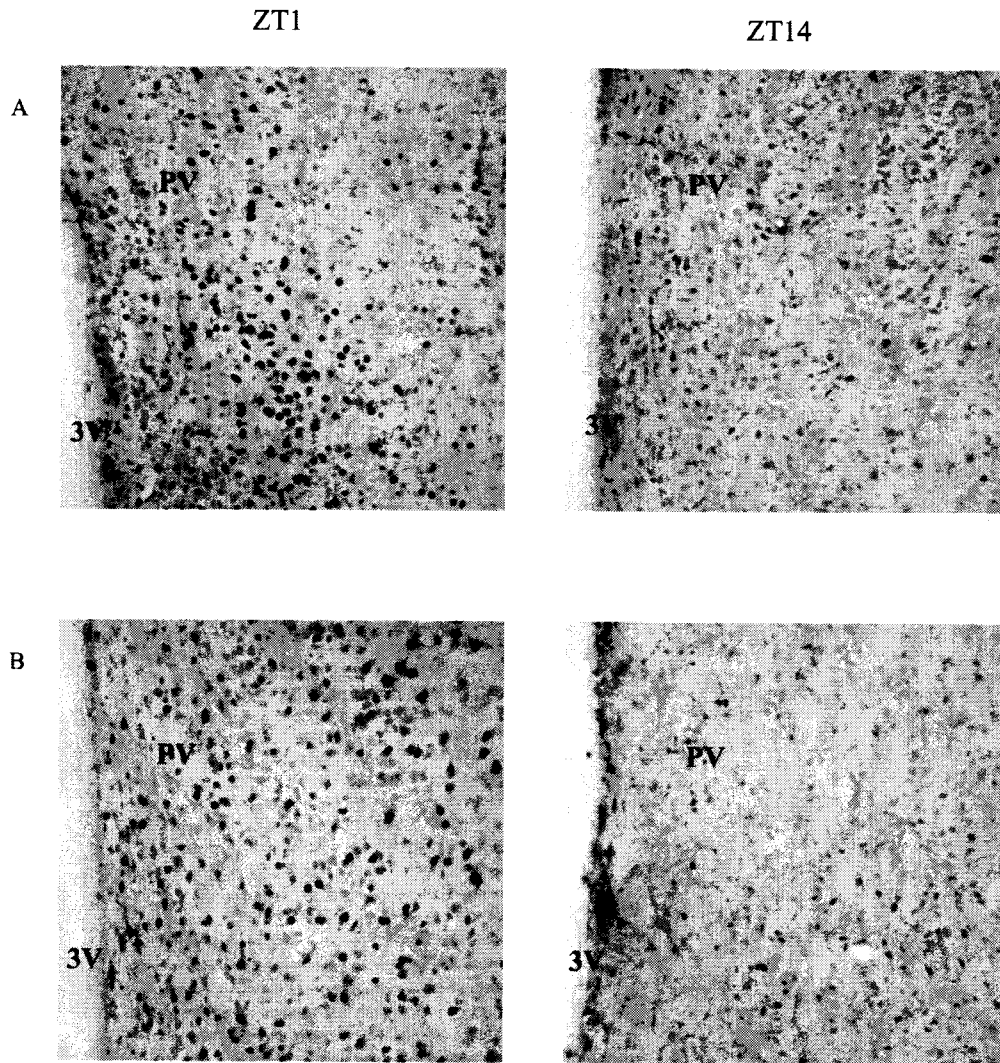


Figure 16. Representative photomicrographs at 10x magnification of PER2-ir cells in the PV of a sham (A, top panels) and a 6-OHDA lesioned rat (B, bottom panels) at ZT1 (left panels) and ZT14 (right panels). 3V = third ventricle, PV = periventricular nucleus.

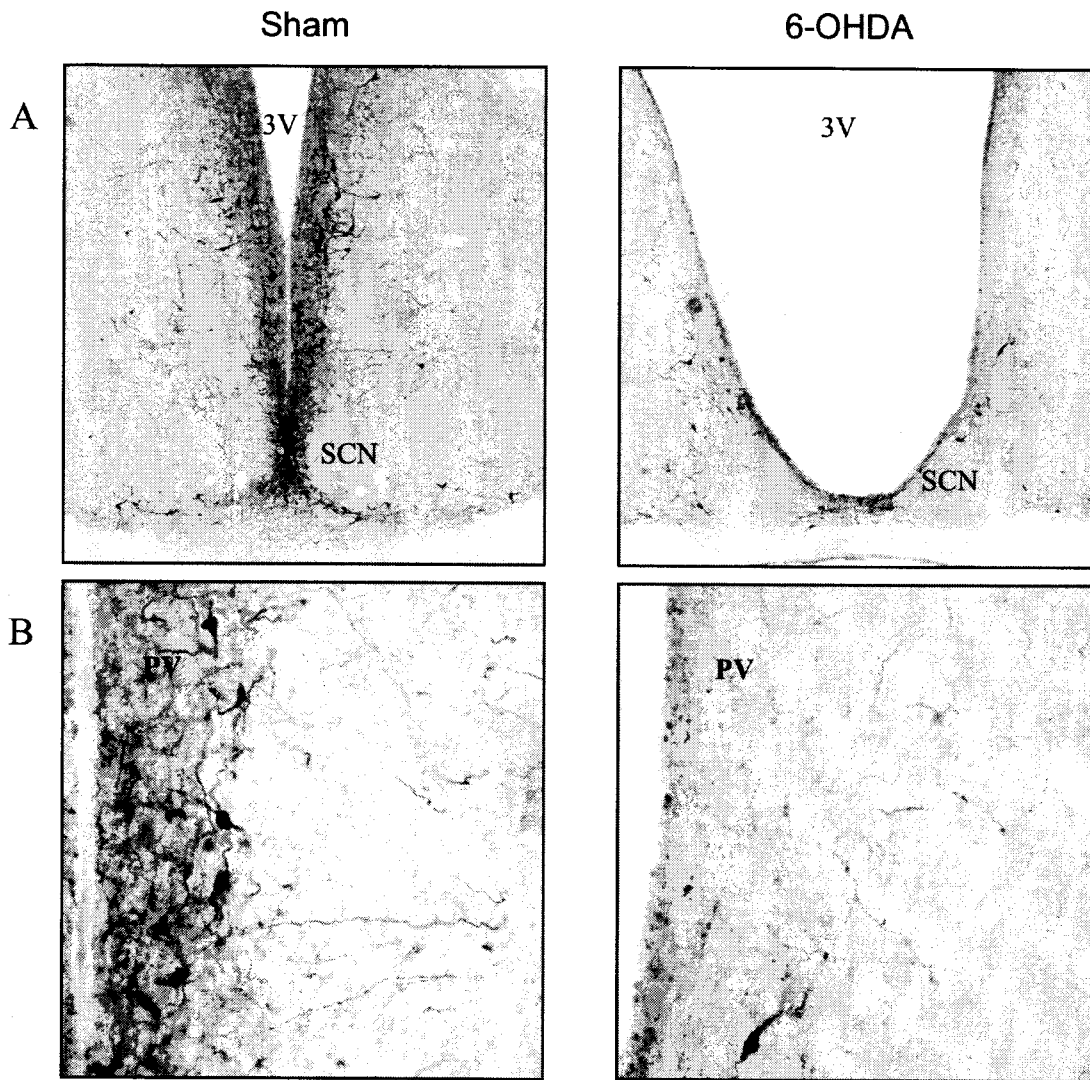


Figure 17. Representative photomicrographs of TH-ir cells and fibers in the periventricular nucleus of a sham (left panels) and a 6-OHDA lesioned (right panels) rat at 5x (A, upper panels) and 10x (B, lower panels) magnification. 3V = third ventricle, SCN = suprachiasmatic nucleus, PV = periventricular nucleus.

Is there a relationship between the blunted activity rhythm observed post-surgery and a) the extent of the lesion in the PV or b) the degree of blunting of PER2 expression (at ZT1) in the PV?

a) In order to investigate if there is a relationship between the blunted activity rhythms and the extent of the lesion in the PV, we used an independent samples t-test to compare the number of TH-ir cells in the PV of 6-OHDA group rats that showed blunted activity rhythms with the number of TH-ir cells in the PV of 6-OHDA group rats that showed normal activity rhythms. We found no significant differences between these two groups ($t(9) = 1.337, p > .05$).

b) In order to investigate the relationship between blunted activity rhythms and PER2 expression, we used an independent samples t-test to compare the number of PER2-ir cells in the PV of 6-OHDA groups rats that showed blunted activity rhythms with the number of PER2-ir cells in the PV of 6-OHDA group rats those that showed normal activity rhythms. We found no significant differences between these two groups ($t(3) = -.279, p > .05$).

Nucleus Accumbens

Qualitative analyses of the Acc of 6-OHDA group rats revealed that the Acc, like the striatum, displayed a variable amount of depletion of TH-ir fibers, with some rats displaying very little depletion, others displaying a large depletion, and still others displaying a lateralized depletion of TH-ir fibers.

Substantia Nigra Pars compacta (SNc)

Figure 18 shows representative photomicrographs of both sham and a 6-OHDA group rats. Our qualitative analysis revealed that, when compared to sham group rats, 9/17 6-OHDA rats had a large reduction of TH-ir fibers and cell bodies in the SNc. 3/17 6-OHDA rats displayed a reduction of TH-ir fibers and cell bodies but this reduction was not as great as that in the aforementioned rats. 5/17 6-OHDA rats were no different from sham group rats in the density of TH-ir fibers and number of cell bodies.

VTA

TH

Qualitative analysis of TH-ir fibers in the VTA revealed that 12/17 of the 6-OHDA rats had large depletion of TH-ir fibers in the VTA while 5/17 of the 6-OHDA rats displayed TH-ir fibers density that was not very different from sham rats (see figure 18). Thus, the number of rats displaying a reduction in TH-ir fiber density and the number of rats displaying no reduction in TH-ir fiber density are the same in both the VTA and the SNc.

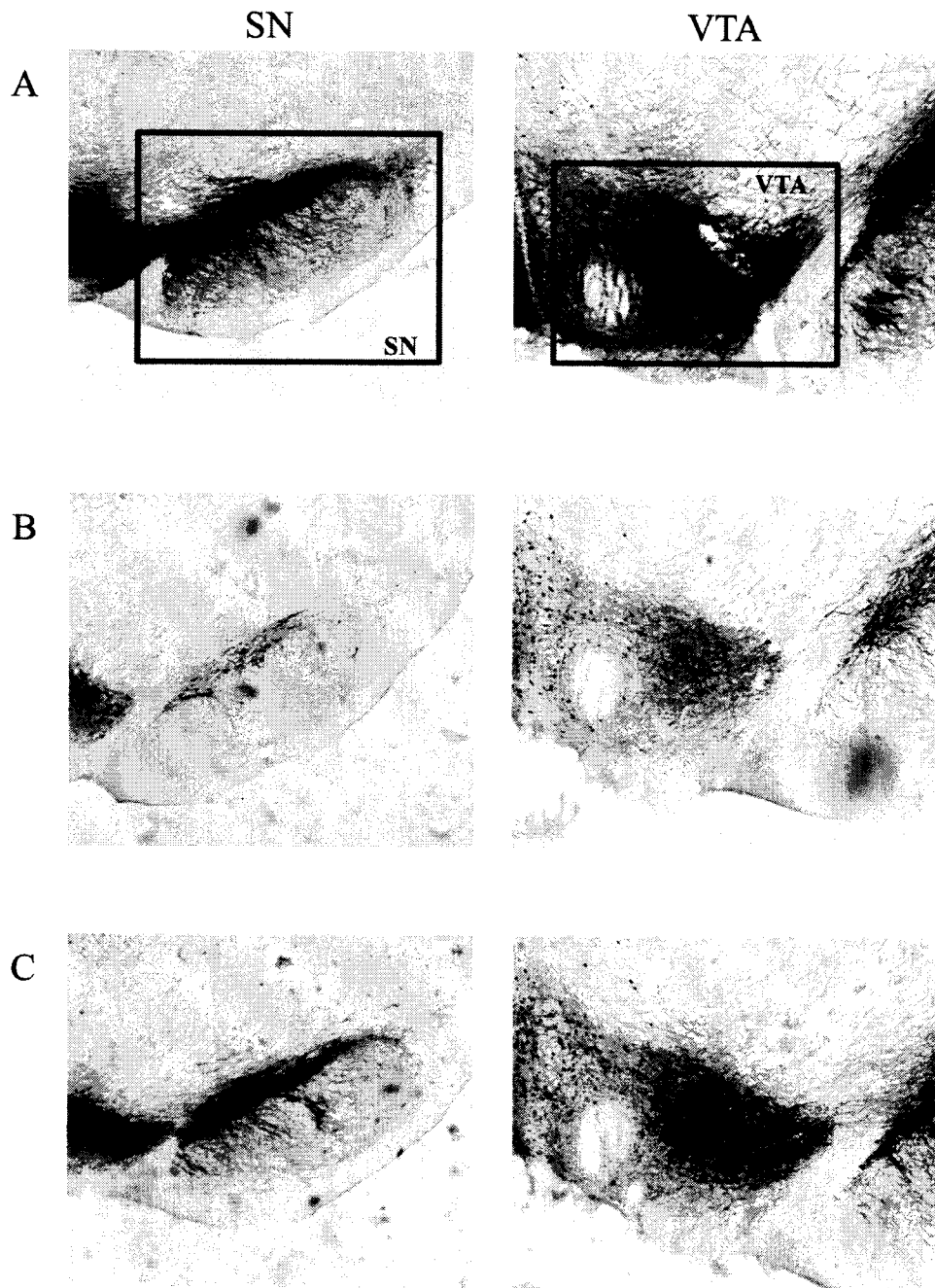


Figure 18. Representative photomicrographs at 5x magnification of TH-ir cells and fibers in the SN and in the VTA of a sham rat (A, top panels), a 6-OHDA lesioned rat with a greater depletion (B, middle panels), and a 6-OHDA lesioned rat with a lesser depletion (C, bottom panels) of TH-ir cells and fibers.

Qualitative analysis and comparison of TH-ir axon terminals and cell bodies in the Striatum, SNc, Acc, VTA, BNSTov and CEA

As previously mentioned, not all rats with 6-OHDA lesions exhibited the same extent of TH-ir fiber depletion. When a rat with a greater lesion was compared to a rat with a lesser lesion, there was a clear pattern of depletion between all the areas examined. Figure 19 shows the six areas of interest in a rat with a lesser lesion and alongside these same areas in a rat with a greater lesion. In the striatum, the lesser lesioned rat displays a darker stain than the greater lesion rat due to the presence of more TH-ir fibers. This same pattern is seen in the SNc, VTA, Acc, BNSTov, and CE. Qualitative analysis of these regions in a rat that had an uneven lesion where the left hemisphere had a much larger depletion in TH-ir fibers than the right hemisphere revealed the same pattern. The same difference in the density of TH-ir fibers between the right and left hemispheres was observed in all six areas examined. These observations indicate that these six areas are all equally affected by the 6-OHDA lesion.

6-OHDA, less depletion

6-OHDA, more depletion

A



B



C



D



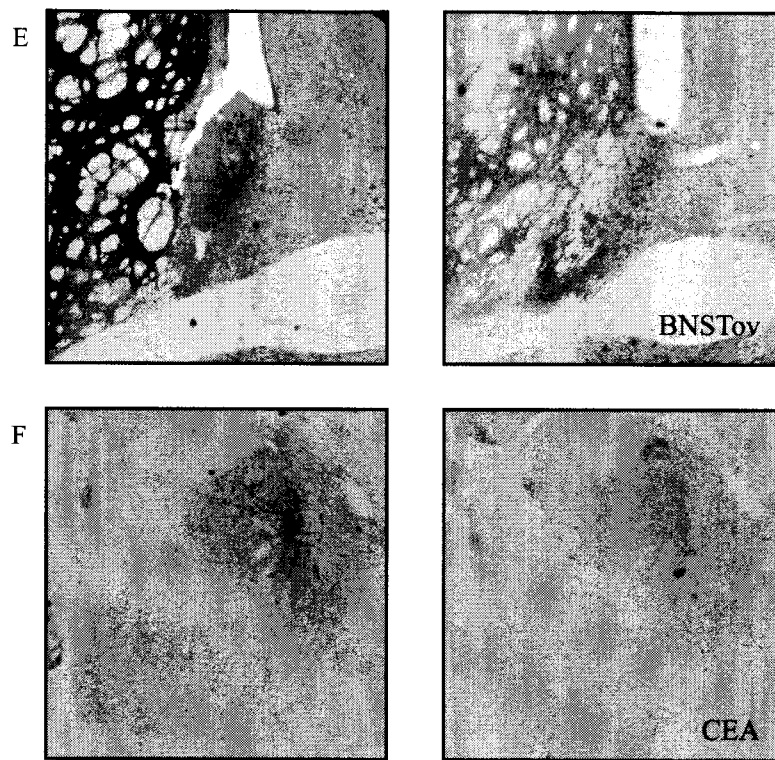


Figure 19. Representative photomicrographs at 5x magnification of TH-ir cells in the striatum (A), SN (B), VTA (C), Acc (D), BNSTov (E), and CEA (F) for a 6-OHDA lesioned rat with less depletion of TH-ir fibers (left panels) and a 6-OHDA lesioned rat with a larger depletion of TH-ir fibers (right panels).

DISCUSSION

The work in this thesis was conducted in order to determine the effect of bilateral (almost global) depletion of dopamine on PER2 expression in the striatum, BNSTov, BLA, CEA, and HC. This work aimed to confirm and extend previous studies in our lab that employ a commonly used technique (*unilateral* dopamine depletion through a unilateral injection of 6-OHDA into the MFB) by employing a less common technique (*bilateral* dopamine depletion through i.c.v. injection of 6-OHDA into the third ventricle). We found that i.c.v. 6-OHDA administration was effective in bilateral depletion of dopamine and that, as seen with unilateral application of 6-OHDA, it blunted the rhythm of PER2 expression in the striatum and the BNSTov. However, unlike the unilateral technique, i.c.v. 6-OHDA resulted in severe behavioral deficits (e.g., akinesia, adipsia, aphagia) as well as a transient effect on the circadian organization of activity rhythms.

A further aim of the present work was to determine the effect of periventricular dopamine depletion on PER2 expression in the SCN. Our analyses of the area immediately dorsal to the SCN revealed a novel pattern of PER2 expression in the PV; we found that in the PV of sham treated rats, there is much greater expression of PER2 at ZT1 than at ZT14, suggestive of a rhythm of PER2 expression in this area. With i.c.v. administration of 6-OHDA we were able to reduce the number of TH-ir neurons found in the periventricular nucleus (PV), and this treatment resulted in blunted PER2 expression in the PV. However, there was no effect on PER2 expression in the SCN.

The results of this thesis demonstrate that dopamine can modulate the circadian rhythm of PER2 expression in the striatum and the BNSTov and that dopamine depletion disrupts the organization of circadian activity rhythms. Furthermore, these results reveal a novel pattern of PER2 expression in the PV, which is blunted after dopamine depletion. Finally, these results corroborate and extend previous work (Ungerstedt, 1971b; Marshall, Richardson, & Teitelbaum, 1974) by describing the behavioral deficits that result from near-global dopamine depletion in the brain.

In this section, we first discuss some of the behavioral deficits observed immediately post surgery and in the weeks prior to perfusion, as these data were obtained prior to any of the immunohistochemical analyses. We then focus on the PV, the SCN, and the observed disruptions in the circadian organization of activity rhythms. We continue with a discussion of the putative mechanism of action of 6-OHDA and the possible routes by which this neurotoxin affected dopamine in the areas of interest in the present paradigm, as well as the link between loss of dopaminergic input and blunted PER2 expression in specific areas. Finally, we discuss the results of the present study in the context of the recent literature on the links between clock genes, mood disorders, PD, and dopamine.

Behavioral Abnormalities

Although early studies report on the severity of behavioral abnormalities (e.g., the absence of drinking (adipsia), the absence of eating (aphagia), and the absence of movement (akinesia)) that result from bilateral depletion of striatal dopamine

(Ungerstedt, 1971b), this is inconsistent with more recent studies (Rodriguez, Barroso-Chinea, Abdala, Obeso & Gonzalez-Hernandez, 2001; Rey et al., 2007). The present study confirms that adipsia, aphagia and akinesia result from the near global depletion of dopamine obtained with the bilateral 6-OHDA lesion and, as described by Ungerstedt (1971b), the adipsia and aphagia are so severe that animals that are not tube-fed, and do not resume eating on their own die within 4-5 days. The severity of these behavioral abnormalities is directly proportional to the extent of the lesion in the striatum. In a series of lesion experiments, Ungerstedt showed that any kind of lesion that depletes dopaminergic terminals in the striatum results in severe adipsia and aphagia, but that no adipsia nor aphagia is observed if the lesion is incomplete (e.g., when some DA innervation to the striatum remains or when there is only unilateral damage), or if the lesion affects only noradrenergic neurons. Similarly, in the present study, rats with the most severe adipsia and aphagia were those with the most extensive TH-ir fiber depletion in the striatum. Adipsia and aphagia have previously been attributed to damage of the lateral hypothalamus, and it was postulated that these deficits resulted from the interruption of afferent connections from the pallidum (Marshall & Richardson, 1974). However, Ungerstedt compared behavioral deficits of rats that had received electrocoagulation or 6-OHDA in either the lateral hypothalamus or the MFB. He observed that lateral hypothalamic lesions, like MFB lesions, resulted in a near-total depletion of dopaminergic fibers in the striatum. Furthermore, in both cases, as previously mentioned, the extent of the striatal lesion was positively correlated with the extent of adipsia and aphagia (Ungerstedt, 1971b). The author concludes from these

observations that adipsia and aphagia are a result of damage to the nigro-striatal dopaminergic pathway.

As the striatum is not traditionally considered to be involved in the regulation of physiological drives, it is most probable that the deficits encountered in these studies are due to a dampening of motivational drive. This, as well as the reduced dopaminergic input to the striatum from the SNc that results in an inhibition of movement (Albin, Young, & Penny, 1989), could also be an explanation for the akinesia observed in these animals. Both in the present study and in Ungerstedt's experiments animals that were mostly akinetic could be made to react by handling or probing them. Thus animals were capable of movement, but the motivation to move or to approach stimuli was deficient. Also in parallel to the present study, Ungerstedt observed that in the first few days following bilateral injection of 6-OHDA into the SN, animals displayed 'motor explosions' (Ungerstedt, 1971b) in response to sudden sounds. Our study further qualifies these 'motor explosions' with the observation that they resembled extremely uncoordinated and uncontrolled flee responses, that at times included abnormal sudden extensions of the hind legs resulting in a 'hopping' behaviour. It has been shown that during movement, some neurons in the internal Globus Pallidus (GPi), one of the output nuclei of the basal ganglia, respond with a phasic decrease while others respond with phasic increase of their normally high rate of discharge (Alexander & Crutcher, 1990). It is thought that these correspond to the facilitation of certain movements and the inhibition of opposing movements in order to achieve fluidity of movement. Disruption of the main input of the GPi, i.e., the striatum, would most probably result in a disruption of these mechanisms for the execution of fluid movements and may explain the

uncoordinated responses observed in the present study. Ungerstedt (1971b) hypothesizes that these responses could be caused by the random release of dopamine into the striatum by degenerating dopaminergic neurons. However, in our study, the hopping behaviour continued to be observed even after the time during which dopaminergic neurons are believed to have completed the process of degeneration in response to 6-OHDA (Zuch, 2000) and once the 'motor explosions' had subsided. The exact cause of this abnormal behaviour thus remains to be elucidated.

PER2 expression in the PV and SCN

To our knowledge, this is the first demonstration of a daily variation of PER2 in the PV of male nocturnal rats (see figure 15). Previous studies have shown a rhythm of PER2 in the PV of ovariectomized female rats (Sellix et al., 2006). However, Sellix and colleagues used drinking and feeding behaviors as markers of circadian time and found the peak and trough of PER2 to be CT6 and CT0, respectively, whereas the current work used zeitgeber time as the marker of circadian time and observed significantly higher levels of PER2 at ZT1 than at ZT14. In the diurnal grass rat, Ramanathan and colleagues (2006) found a rhythm of PER2 and PER1 expression in the lower subparaventricular zone (LSPV), the area equivalent to the PV in the rat. The authors report a peak at ZT10 and a trough at ZT0-6 for both proteins in the male, and a peak at ZT10 and a trough at ZT18 of PER1 in the female (Ramanathan et al., 2006). In mice, Kriegsfeld and colleagues (2003) found that the antero-ventral periventricular area (AVPV), an area equivalent to the PV, expressed *per1* and PER1, however, they did not detect a rhythm of protein expression in this area (Kriegsfeld, Korets, & Silver, 2003). Thus, in the absence

of any contrary data, we propose that the PV in the male rat displays a daily variation in PER2 expression with high levels of expression at ZT1 and low levels of expression at ZT14.

We also showed that i.c.v. 6-OHDA results in a decrease in the number of TH-ir cells in the PV (see figure 15). Although this area is one of the seventeen cell groups of catecholamine neurons (Bjorklund & Dunnett, 2007), it is not considered to be a dopaminergic cell group. The PV is immunopositive for TH but not for aromatic L-aminoacid decarboxylase (AADC) and thus lacks the enzyme necessary for converting L-DOPA to DA (Bjorklund & Dunnett, 2007). However, loss of TH-ir cells could have implications for L-DOPA signaling to the SCN, which as discussed in the introduction, could be converted to DA in the AADC-ir SCN cells (Ishida et al., 2002) and affect SCN function through D1 receptors localized on SCN cells (Fremeau et al., 1991, Ishida et al., 2002). Although there was a clear reduction in the density of TH-ir cells and fibers in the PV and this was associated with a decrease in PER2 expression at ZT1, there was no effect of PV TH-ir cell loss on the PER2 rhythm in the SCN. Note that although only two time points were analyzed (i.e., ZT1 and ZT14) we say that PER2 expression is rhythmic because the rhythm of PER2 expression in the SCN and many other extra-SCN oscillators has been extensively characterized, i.e., PER2 expression measured every half hour for 24 hours (Harbour, unpublished results), with the SCN displaying its trough and peak of PER2 expression at ~ZT1 and ~ZT14, respectively.

It is still unclear how circadian genes are regulated in the PV and the nature of the interaction between the SCN and the PV. Sellix and colleagues have demonstrated that disruption of clock gene (*per1/2* and *clock*) rhythms in the SCN through antisense

knockdown disrupts the circadian rhythm of dopamine turnover normally observed in the PV (in OVX female rats), advancing the peak by six hours and increasing the amount of DA turnover at CT15. The treatment also dampened PER1/PER2 and CLOCK expression in the PV (Sellix et al., 2006). It has also been suggested that the PV can play a role in the synchronization of neurons in the SCN. Battaglia and colleagues (1995) have shown that in young rats (PD10), TH-ir cells in the PV have axons that run ventrally towards the SCN and that some of the TH-ir fibers that surround the SCN make contact with VIP-ir neurons in the SCN, suggesting a possible mechanism by which L-DOPA could be delivered to the SCN and influence VIP, which is important in the synchronization of clock gene rhythms in the neurons of the SCN (Battaglia, Beltramo, Thibault, Krieger, & Calas, 1995).

In the present study we observed a transient disorganization of the circadian rhythm of locomotor activity that revealed itself as soon as the 6-OHDA treated animals resumed activity post-surgery. Our lab has previously demonstrated that transient suppression of PER2 production in the SCN through RNA interference leads to a disruption of circadian locomotor activity (Gavrila et al., 2008). This and other work (LeSauter & Silver, 1998) show the critical role of the SCN in the regulation of circadian locomotor activity rhythms. However, the present study observed a disorganization of activity rhythms with no disruption of PER2 expression in the SCN. It is possible that PER2 expression was disrupted in the SCN only transiently (i.e., when disorganized activity rhythms were observed). However, as animals were sacrificed once they were put back on a LD schedule and had re-entrained, we cannot conclude whether or not disorganized activity rhythms reflect an underlying disruption in PER2 expression in the

SCN. Further studies are needed in order to determine whether, as observed in the present study, dopamine depletion results in a disruption of activity rhythms that is not accompanied by a disruption of PER2 expression in the SCN. If a dissociation between PER2 expression in the SCN and behavioral output were to be observed in future studies, it would suggest that extra-SCN structures are involved in the observed disorganization of activity rhythms.

Based on the present data and on previous studies (Weaver & Reppert, 1995), it seems that although the SCN may be responsive to PV innervation in young rats (Battaglia, Beltramo, Thibault, Krieger, & Calas, 1995), and to DA signaling in neonatal rats (Weaver & Reppert, 1995; Grosse & Davis, 1999), the SCN loses this responsiveness in adult rats. It is possible that the observed disorganization in locomotor activity rhythms could be a result of the depletion of dopamine and the blunted rhythm of PER2 expression in the striatum. PD patients who show a degeneration of dopaminergic neurons in the SNc and a resulting decrease of DA in the striatum often have sleep problems such as daytime sleepiness, parasomnia, fragmented sleep, and insomnia (Bruguerolle & Simon, 2002; Gunn, Naismith, & Lewis, 2010). Furthermore, a small clinical trial with 9 PD patients observed a phase advance in the peak of serum melatonin levels of PD patients when compared to healthy controls. Note however, that the subjects in this study received daily L-Dopa treatment, which could be responsible for the shift in the peak (Bruguerolle & Simon, 2002). These studies demonstrate abnormalities in both physiological and behavioral rhythms (Fertl, Doppelbauer, & Waldhauser, 1991). It is possible that in the present study the depletion of dopamine may have caused similar symptoms in the 6-OHDA lesioned rats resulting in an abnormal pattern of rhythmic

activity characterized by activity during the subjective light phase when rats are normally inactive (see figures 2 and 4). Another possibility is that the dopaminergic denervation-induced blunting of the PER2 rhythm in the striatum results in the observed disorganized activity pattern. Iijima (2002) and colleagues have shown that circadian activity rhythms can be entrained to daily methamphetamine injections. This treatment does not affect *Per1* nor *Per2* gene expression in the SCN but does shift the expression of these genes in the striatum, and this shift is correlated with the shift in activity rhythms. This study suggests that clock gene expression in the striatum is involved in the production of rhythms of locomotor activity (McClung, 2007). If striatal dopamine depletion and the subsequent blunting of PER2 expression is the cause of this behavior, what remains unclear is why this behavior is transient. The severe loss of dopaminergic innervation in the striatum and the reduction in PER2 counts were observed weeks after the disorganized activity rhythms returned to normal. Thus, the recovery of organized activity rhythms cannot be attributed to the recuperation of dopaminergic input nor to the recuperation of the normal rhythmic expression of PER2. It is possible that yet to be described compensatory mechanisms play a role in the recovery of organized activity rhythms.

To summarize, dopamine can affect the expression of PER2 in the PV, but the loss of TH-ir cells and the reduction in PER2 expression in this area have no effect on rhythmic expression of PER2 in the SCN. Although it remains to be elucidated whether the observed behavioral abnormalities are a result of the disruption of PER2 expression in the striatum, it is clear that the loss of endogenous striatal dopamine plays a role in the appearance of these abnormalities.

Intraventricular 6-OHDA: mode of action

In the present work, i.c.v. administration of 6-OHDA resulted in the depletion of dopamine not only in the striatum but in other areas as well. The neurotoxin 6-OHDA is taken up by DA and NE cells through transmembrane transporters (Nass, et al. 2005). In the present study, desipramine was used to protect NE cells from 6-OHDA induced damage. Desipramine inhibits re-uptake of NE by blocking NE transporters. By blocking NE transporters, desipramine also blocks uptake of 6-OHDA into NE cells (Lindvall, Bjorklund, & Skagerberg, 1984). If the neurotoxin is injected near cell terminals (as it was in this case), or into fibers of passage (as it is in unilateral lesions targeting the MFB), the neurotoxin can reach the fiber's somatic origin by means of retrograde transport (Zuch et al., 2000). If the neurotoxin is injected near cell bodies, it can reach the nerve terminals by means of anterograde transport (Ungerstedt, 1971b). The putative mechanism by which 6-OHDA is thought to damage neurons and neuronal fibers is through the creation of free-radicals and oxidative elements inside the neuron which then damage the neuron and lead to cell death (Ungerstedt, 1971b; Zuch et al., 2000; Marianova-Mutafchieva et al., 2009). Neurotoxic induced degeneration of the DA neurons has been established as apoptotic rather than necrotic (Zuch et al., 2000), and microglial activation and proliferation has been associated with the loss of TH-ip cells in the SNc (Marianova-Mutafchieva et al., 2009).

As the VTA and SNc send dopaminergic projections to the dorsal and ventral striatum, respectively (Ungerstedt, 1971; Moore & Bloom, 1978; Bjorklund & Dunnett, 2007), the clear reduction in dopaminergic fibers and cell bodies in the VTA and SNc in most of the 6-OHDA animals can be attributed to retrograde transport of the neurotoxin

from the Acc and the striatum. This conclusion is further supported by the fact that the Acc and the striatum themselves show an extensive reduction in dopaminergic fibers. Interestingly, although the present study and others that have used i.c.v. administration of 6-OHDA report a reduction in dopaminergic cell fibers in the SNc and the VTA (Rodriguez, Barroso-Chinea, Abdala, Obeso, & Gonzalez-Hernandez, 2001), there is no consensus on the effect of a unilateral injection of 6-OHDA into the MFB on the VTA. Our lab has observed unilateral degeneration of dopamine transporter (DAT) immunoreactive fibers in the VTA and Acc (Hood, unpublished results) while Marinova-Mutafchieva (2008) and colleagues report a unilateral reduction in dopaminergic cell fibers in the SNc but no reduction in the VTA. In the case of the unilateral lesion, it is possible that injection into the MFB can affect the fibers that run from the VTA to the NAcc as these are located in the MFB and run parallel to the fibers that run from the SNc to the striatum. In the case of i.c.v. administration of 6-OHDA, as the Acc lies adjacent to the lateral ventricle, diffusion of the neurotoxin throughout the ventricular system could result in its uptake by the dopaminergic fibers in the Acc and retrograde transport to cell bodies in the VTA resulting in the degradation of dopaminergic cell bodies and fibers in these areas. Thus, it seems that although the putative mechanisms by which the unilateral and i.c.v. techniques cause degeneration in the mesostriatal system differ, both may result in the degeneration of dopaminergic cell bodies and fibers in the same areas (albeit the degeneration is bilateral and not unilateral in the case of the i.c.v. technique).

Loss of dopaminergic afferents, changes in PER2 expression: striatum, BNSTov, and CEA.

The loss of dopaminergic afferents to the striatum was clearly associated with a blunting of rhythmic expression of PER2 in the striatum. As previously mentioned in the case of the SCN, we refer to a rhythm in the striatum even though we only analyzed two time points. Our lab has already characterized the striatal rhythm of PER2 expression, establishing that the peak occurs between ZT23-1 and the trough occurs between ZT10-14 (Harbour, unpublished data). Thus we use ZT1 and ZT14 as representative of the rhythm. In all regions examined, the decrease in dopaminergic afferents had no effect on the trough of PER2 expression, however, it dramatically attenuated the peak of PER2 expression (see figure 9). Interestingly, when comparing the anterior with the posterior striatum of 6-OHDA lesioned rats, we observed differences in the relative levels of PER2 expression at ZT1 and ZT14. In the anterior striatum, although PER2 levels were blunted at ZT1 compared to sham rats, 6-OHDA rats had significantly higher levels of PER2 expression at ZT1 than at ZT14. On the other hand, in the posterior striatum, 6-OHDA rats showed no significant difference in PER2 levels between ZT1 and ZT14. These results suggest that the anterior striatum retained rhythmic yet blunted expression of PER2 but that the posterior striatum lost rhythmic expression of PER2, and instead expressed constant levels of the protein. An alternative explanation for these differences could be that as the posterior striatum displays a lower amplitude in the rhythm of PER2 expression than that of the anterior striatum (Harbour, unpublished results), an equal amount of blunting in the two areas could result in a blunted difference in the number of PER2-ir cells between the peak and trough in the anterior striatum and a disappearance of

a difference in the number of PER2-ir cells between the peak and the trough in the posterior striatum.

As observed previously in our lab with the unilateral 6-OHDA lesion (Hood, unpublished results), here we show that i.c.v. 6-OHDA administration resulted in a reduction of TH-ir fibers and a blunting of the PER2 rhythm in the BNSTov. As the BNSTov lies adjacent to the lateral ventricles, one explanation for the loss of TH-ir fibers might be that diffusion of 6-OHDA throughout the ventricles results in a depletion of the dopaminergic fibers in this area. Another pathway through which 6-OHDA could damage dopaminergic fibers in the BNSTov is by destruction or impairment of a direct dopaminergic pathway. Tracing and lesion studies have shown that the BNSTov receives innervation from the VTA (Phelix, Liposits, & Paull, 1992), that the BNST receives input from the PV (Moore & Bloom, 1978), and that dopaminergic axons enter the BNST through the MFB (Ungerstedt, 1971a). In the present study we show that i.c.v. 6-OHDA results in depletion of dopaminergic fibers and cell bodies in the SNc and the VTA as well as the depletion of TH-ir fibers and cell bodies in the PV. Thus, it is likely that the depletion of dopaminergic fibers in the BNSTov is the result of the degradation of dopaminergic cells in these areas that project to the BNSTov. Interestingly, our lab has shown that rats that receive daily injections of quinpirole, a DA agonist, at ZT1 for 10 days show a slight increase of PER2 expression at ZT1 in the BNSTov (Hood, unpublished results). This data fits well with the present results, suggesting that in the BNSTov increases in endogenous DA lead to an increase of peak PER2 expression and decreases in endogenous DA lead to a decrease of peak PER2 expression.

Unlike the BNSTov, the CEA did not display a blunted PER2 rhythm. However, i.c.v. administration of 6-OHDA did result in a depletion of dopaminergic fibers in the CEA in most of the animals who received this treatment. Tracing and lesion studies show that the CEA receives dopaminergic input from the the SNc (Moore & Bloom, 1978). The pathway from the SNc to the CEA is the same as that from the SNc to the striatum (Ungerstedt, 1971a). Thus, it is likely that the reduction in dopaminergic cells and fibers in the SNc led to a depletion in dopaminergic input to the CEA. However, it is still unclear why depletion of dopaminergic input led to a blunting of the PER2 rhythm in the BNSTov, but not in the CEA. It is important to note that in both sham rats and 6-OHDA rats the density of TH-ir fibers is much greater in the BNSTov than it is in the CEA.

Desynchrony between the SCN and extra-SCN clocks: implications

The blunted rhythms of PER2 expression observed in the striatum and the BNSTov in response to the depletion of dopaminergic afferents to these areas demonstrates that dopamine has a modulatory role in the expression of PER2 in these regions. As part of the basal ganglia, the striatum is involved in the regulation of voluntary motor movements (Albin, Young & Penney, 1989; DeLong & Wichmann, 2009) and as part of the extended amygdala, the BNST is believed to be involved in fear and anxiety like behaviors (Pezuk, Goz, Aksoy & Canbeyli, 2006; Resstel et al., 2008). The disruption in the rhythm of PER2, an essential protein that provides negative feedback to the molecular clock, can presumably have negative consequences on the functioning of these areas. Desynchrony between the SCN and extra-SCN clocks, i.e. changes in the coupling between oscillating clock gene expression in certain regions, has

been linked to adverse health consequences. For example it has been found that the prevalence of cancer, cardiovascular disease, and gastrointestinal disease is higher in shift workers, whose behavioral rhythms (e.g., eating, sleeping) are not synchronized to environmental time cues (e.g., daylight) resulting in a desynchronisation between the master clock and peripheral clocks (e.g., the liver) (Hastings, Reddy & Maywood, 2003). Furthermore, as previously mentioned, since the interaction between DA and clock gene expression is reciprocal, this disruption of PER2 can lead to further dysregulation of DA signaling. For example, in the striatum the peak of PER2 at ZT1 results in an increase in MAOA and in turn, this leads to a decrease in DA levels. Thus, disruption of the PER2 peak may affect MAOA expression and lead to altered DA levels (Hempp, 2008).

A link between the dopamine system and clock gene expression in extra-SCN oscillators in the context of mood disorders and Parkinson's disease

Our work, which shows a link between the dopamine system and clock gene expression in extra-SCN oscillators, is also relevant in the context of the recent literature, which shows links between mood disorders and the circadian system (Lamont et al., 2007) and between Parkinson's disease and the circadian system (Bruguerolle & Simon, 2002). Mood disorders, such as major depressive disorder (MDD), bipolar disorder (BPD), and schizophrenia, are thought to be caused by a dysregulation of dopamine systems in the brain (Abi-Dargham, 2004; Nestler & Carlezon, 2006). Abnormalities in sleep-wake patterns such as insomnia, early morning awakenings (implicating a phase advance of the endogenous period), as well as in the circadian rhythm of hormone levels (e.g., cortisol) have been implicated in these disorders (Lamont et al., 2007). It is still

unclear whether mood disorders lead to disturbances of circadian rhythms or whether dysregulated circadian rhythms are a factor in the etiology of these disorders. Some studies suggest a link between polymorphisms in the CLOCK gene and both BPD and schizophrenia (Lamont et al., 2007; Takao et al., 2007). Furthermore, treatments that shift or normalize circadian rhythms such as light therapy, total sleep deprivation, and strict adherence to a daily schedule where the patient gets up and goes to sleep at the same time everyday, have been shown to be effective in mood stabilization in both depression and BPD (McClung, 2007). Of particular interest to the present discussion is the effect of lithium on circadian rhythms. Lithium has been widely used for treatment of BPD and it has been shown to modulate the phase and period of circadian rhythms (Gould & Manji, 2005). Studies suggest that lithium inhibits the activity of the enzyme, glycogen synthase kinase-3 (GSK-3), and that this inhibition is responsible for the effects of lithium on mood (Gould & Manji, 2005). Other mood-stabilizing drugs have been found to target GSK-3 as well. Interestingly, GSK-3 plays a role in the regulation of clock genes through phosphorylation of PER and CRY proteins (Falcon & McClung, 2009) as well as in the regulation of dopaminergic signaling (Gould & Manji, 2005). These findings suggest a common pathway for the regulation of both dopamine signaling and circadian genes.

Also relevant to the present work is recent research on the relationship between Parkinson's disease and circadian rhythms (Bruguerolle & Simon, 2002). As previously mentioned, the main feature of PD is the degeneration of the dopaminergic neurons in the substantia nigra and a loss of dopamine input to the striatum that lead mainly to deficits in motor function (DeLong & Wichmann, 2009). However, circadian and mood abnormalities are also present in patients with PD. PD patients suffer from sleep

problems such as fragmented sleep and insomnia, and disruptions in autonomic circadian rhythms such as the rhythm of blood pressure (Brugueroll & Simon, 2002). Recently, Cai and colleagues (2009) have shown that compared to control subjects, BMAL1 expression in leukocytes of PD patients is significantly lower at certain time points. Fukuya and colleagues (2007) however, find that there is no rhythm of *Bmal1* in the leukocytes of healthy subjects. Thus, no conclusions can yet be drawn regarding clock gene expression in PD. Forty percent of PD patients suffer from major depressive disorder and several lines of evidence point to the dysregulation of dopamine in several brain areas as the cause of this mood disorder (Stocchi & Brusa, 2000). Given the symptoms of sleep and circadian abnormalities and of mood disorder in this disease thought to be caused by the degeneration of dopaminergic areas of the brain, and in light of the previous discussion linking mood disorders and dopamine to clock genes, it is interesting to speculate whether abnormal clock gene expression in extra-SCN brain regions may also play a role in the symptomology of PD. The unilateral 6-OHDA lesion has been widely used to model PD in rodents (Schwartz & Huston, 1996; Simola, Morelli, & Carta, 2007) and the areas in which dopamine depletion is observed with i.c.v. 6-OHDA injections are the same as the areas in which dopamine depletion is observed in PD patients (Rodriguez, Barroso-Chineas, Abdala, Obeso, & Gonzalez-Hernandez, 2001). Thus based on our findings, we suggest that there is a strong link between dopamine and clock genes in extra-SCN areas. However, whether clock genes have a role in the sleep and circadian abnormalities observed in PD remains to be elucidated.

General summary of the conclusions

In conclusion, the present work found a previously unobserved rhythm of PER2 expression in the PV of the nocturnal male rat, and showed that this rhythm was blunted following the loss of TH-ir fibers in the PV. Furthermore, the present work showed that i.c.v. injection of 6-OHDA results in a near-global depletion of dopamine in the brain and a blunting of the PER2 rhythm in the striatum, the BNSTov, and the PV. One goal of the present investigation was to determine if a more widespread disruption of clock genes could be obtained with bilateral (as opposed to unilateral) dopamine depletion. However, blunting of PER2 in the striatum and BNSTov is also observed in unilaterally lesioned rats (Hood, unpublished results). As the abnormal behavioral responses and high mortality rates that result from bilateral dopamine depletion are not observed in studies that employ unilateral administration of 6-OHDA (Schwartz & Huston, 1996; Blandini, Armentero & Martignoni, 2008), we recommend the unilateral technique for the investigation of the interaction between dopamine and clock genes. I.c.v. administration of 6-OHDA, however, is the only method thus far employed to achieve depletion of TH-ir cells and fibers in the PV.

Most importantly, the present work extends the findings from previous studies by our lab and others, showing that dopamine can modulate the expression of PER2 in some areas of the basal ganglia and the extended amygdala, mainly, the striatum and the BNSTov. This connection will be an important element in future work that aims to elucidate the underlying mechanisms responsible for some of the symptomatology of mood disorders and of Parkinson's disease.

REFERENCES

- Abe, M., Herzog, E. D., Yamazaki, S., Straume, M., Tei, H., Sakaki, Y., et al. (2002). Circadian rhythms in isolated brain regions. *J Neurosci*, 22(1), 350-356.
- Abi-Dargham, A. (2004). Do we still believe in the dopamine hypothesis? New data bring new evidence. *Int J Neuropsychopharmacol*, 7 Suppl 1, S1-5.
- Albrecht, U. (2006). Orchestration of gene expression and physiology by the circadian clock. *J Physiol Paris*, 100(5-6), 243-251.
- Alexander. (1990). Functional architecture of basal ganglia circuits: neural substrates of parallel processing. *Trends in Neurosciences*, 1-6.
- Amir, S., Lamont, E. W., Robinson, B., & Stewart, J. (2004). A circadian rhythm in the expression of PERIOD2 protein reveals a novel SCN-controlled oscillator in the oval nucleus of the bed nucleus of the stria terminalis. *J Neurosci*, 24(4), 781-790.
- Andretic, R., & Hirsh, J. (2000). Circadian modulation of dopamine receptor responsiveness in *Drosophila melanogaster*. *Proc Natl Acad Sci USA*, 97(4), 1873-1878.
- Battaglia, A. A., Beltramo, M., Thibault, J., Krieger, M., & Calas, A. (1995). A confocal approach to the morphofunctional characterization of the transient tyrosine hydroxylase system in the rat suprachiasmatic nucleus. *Brain Research*, 696(1-2), 7-14.
- Besharse, J. C., Zhuang, M., Freeman, K., & Fogerty, J. (2004). Regulation of photoreceptor Per1 and Per2 by light, dopamine and a circadian clock. *Eur J Neurosci*, 20(1), 167-174.
- Björklund, A., Lindvall, O., & Nobin, A. (1975). Evidence of an incerto-hypothalamic dopamine neurone system in the rat. *Brain Research*, 89(1), 29-42.
- Björklund, A., & Nobin, A. (1973). Fluorescence histochemical and microspectrofluorometric mapping of dopamine and noradrenaline cell groups in the rat diencephalon. *Brain Research*, 51, 193-205.
- Blum, D., Torch, S., Lambeng, N., Nissou, M., Benabid, A. L., Sadoul, R., et al. (2001). Molecular pathways involved in the neurotoxicity of 6-OHDA, dopamine and MPTP: contribution to the apoptotic theory in Parkinson's disease. *Prog Neurobiol*, 65(2), 135-172.

- Boulos, Z., & Terman, M. (1980). Food availability and daily biological rhythms. *Neuroscience and biobehavioral reviews*, 4(2), 119-131.
- Cahill, G. M., & Besharse, J. C. (1991). Resetting the circadian clock in cultured *Xenopus* eyecups: regulation of retinal melatonin rhythms by light and D2 dopamine receptors. *J Neurosci*, 11(10), 2959-2971.
- Cahill, G. M., & Besharse, J. C. (1993). Circadian clock functions localized in *xenopus* retinal photoreceptors. *Neuron*, 10(4), 573-577.
- Cai, Y., Liu, S., Sothorn, R. B., Xu, S., & Chan, P. (2010). Expression of clock genes *Per1* and *Bmal1* in total leukocytes in health and Parkinson's disease. *Eur J Neurol*, 17(4), 550-554.
- Day, H. E. W., Vittoz, N. M., Oates, M. M., Badiani, A., Watson, S. J., Robinson, T. E., et al. (2002). A 6-hydroxydopamine lesion of the mesostriatal dopamine system decreases the expression of corticotropin releasing hormone and neurotensin mRNAs in the amygdala and bed nucleus of the stria terminalis. *Brain Research*, 945(2), 151-159.
- Delgado, M. R., Li, J., Schiller, D., & Phelps, E. A. (2008). The role of the striatum in aversive learning and aversive prediction errors. *Philos Trans R Soc Lond, B, Biol Sci*, 363(1511), 3787-3800.
- DeLong, M., & Wichmann, T. (2009). Update on models of basal ganglia function and dysfunction. *Parkinsonism Relat Disord*, 15 Suppl 3, S237-240.
- Duffield, G. E., Hastings, M. H., & Ebling, F. J. (1998). Investigation into the regulation of the circadian system by dopamine and melatonin in the adult Siberian hamster (*Phodopus sungorus*). *Journal of Neuroendocrinology*, 10(11), 871-884.
- Fertl, E., Auff, E., Doppelbauer, A., & Waldhauser, F. (1991). Circadian secretion pattern of melatonin in Parkinson's disease. *J Neural Transm Park Dis Dement Sect*, 3(1), 41-47.
- Flores-Barrera, E., Vizcarra-Chacón, B. J., Tapia, D., Bargas, J., & Galarraga, E. (2010). Different corticostriatal integration in spiny projection neurons from direct and indirect pathways. *Front Syst Neurosci*, 4, 15.
- Freneau, R. T., Duncan, G. E., Fornaretto, M. G., Dearry, A., Gingrich, J. A., Breese, G. R., et al. (1991). Localization of D1 dopamine receptor mRNA in brain supports a role in cognitive, affective, and neuroendocrine aspects of dopaminergic neurotransmission. *Proc Natl Acad Sci USA*, 88(9), 3772-3776.
- Girotti, M., Weinberg, M. S., & Spencer, R. L. (2009). Diurnal expression of functional and clock-related genes throughout the rat HPA axis: system-wide shifts in

- response to a restricted feeding schedule. *Am J Physiol Endocrinol Metab*, 296(4), E888-897.
- Golombek, D. A., & Rosenstein, R. E. (2010). Physiology of circadian entrainment. *Physiol Rev*, 90(3), 1063-1102.
- Goudreau, J. L., Falls, W. M., Lookingland, K. J., & Moore, K. E. (1995). Periventricular-hypophysial dopaminergic neurons innervate the intermediate but not the neural lobe of the rat pituitary gland. *Neuroendocrinology*, 62(2), 147-154.
- Gould, T. D., & Manji, H. K. (2005). Glycogen synthase kinase-3: a putative molecular target for lithium mimetic drugs. *Neuropsychopharmacology*, 30(7), 1223-1237.
- Green, D. J., & Gillette, R. (1982). Circadian rhythm of firing rate recorded from single cells in the rat suprachiasmatic brain slice. *Brain Research*, 245(1), 198-200.
- Härfstrand, A., Fuxe, K., Cintra, A., Agnati, L. F., Zini, I., Wikström, A. C., et al. (1986). Glucocorticoid receptor immunoreactivity in monoaminergic neurons of rat brain. *Proc Natl Acad Sci USA*, 83(24), 9779-9783.
- Iijima, M., Nikaido, T., Akiyama, M., Moriya, T., & Shibata, S. (2002). Methamphetamine-induced, suprachiasmatic nucleus-independent circadian rhythms of activity and mPer gene expression in the striatum of the mouse. *Eur J Neurosci*, 16(5), 921-929.
- Ishida, N., Kaneko, M., & Allada, R. (1999). Biological clocks. *Proc Natl Acad Sci USA*, 96(16), 8819-8820.
- Kiss, A., Jezova, D., & Aguilera, G. (1994). Activity of the hypothalamic pituitary adrenal axis and sympathoadrenal system during food and water deprivation in the rat. *Brain Research*, 663(1), 84-92.
- Kosobud, A.E., Gillman, A.G., Leffel, J.K., Pecoraro, N.C., REbec, G.V., & Timberlake, W. (2007). Drugs of abuse can entrain circadian rhythms. *Scientific World Journal*, 7, 203-212.
- Kriegsfeld, L.J., Korets, R., & Silver, R. (2003). Expression of the circadian clock gene Period 1 in neuroendocrine cells: an investigation using mice with a Per1:GFP transgene. *Eur J Neurosci*, 17(2), 212-220.
- Lamont, E. W., Diaz, L. R., Barry-Shaw, J., Stewart, J., & Amir, S. (2005). Daily restricted feeding rescues a rhythm of period2 expression in the arrhythmic suprachiasmatic nucleus. *Neuroscience*, 132(2), 245-248.

- Lamont, E. W., Robinson, B., Stewart, J., & Amir, S. (2005). The central and basolateral nuclei of the amygdala exhibit opposite diurnal rhythms of expression of the clock protein Period2. *Proc Natl Acad Sci USA*, *102*(11), 4180-4184.
- Le Foll, B., Gallo, A., Le Strat Y., Lu, L., & Gorwood, P. (2009). Genetics of dopamine receptors and drug addiction; a comprehensive review. *Behav Pharmacol*, *20*(1), 1-17.
- LeSauter, J., & Silver, R. (1998). Output signals of the SCN. *Chronobiol Int*, *15*(5), 535-550.
- Lindvall, O., Björklund, A., & Skagerberg, G. (1984). Selective histochemical demonstration of dopamine terminal systems in rat di- and telencephalon: new evidence for dopaminergic innervation of hypothalamic neurosecretory nuclei. *Brain Research*, *306*(1-2), 19-30.
- Lonstein, J. S., & Blaustein, J. D. (2004). Immunocytochemical investigation of nuclear progesterin receptor expression within dopaminergic neurones of the female rat brain. *Journal of Neuroendocrinology*, *16*(6), 534-543.
- Marinova-Mutafchieva, L., Sadeghian, M., Broom, L., Davis, J. B., Medhurst, A. D., & Dexter, D. T. (2009). Relationship between microglial activation and dopaminergic neuronal loss in the substantia nigra: a time course study in a 6-hydroxydopamine model of Parkinson's disease. *J Neurochem*, *110*(3), 966-975.
- Marshall, J.F., Richardson, J.S., & Teitelbaum, P. (1974). Nigrostriatal bundle damage and the lateral hypothalamic syndrome. *J Comp Physiol Psychol*, *87*, 808-830.
- McClung, C. A. (2007). Circadian genes, rhythms and the biology of mood disorders. *Pharmacol Ther*, *114*(2), 222-232.
- Meerlo, P., Sgoifo, A., & Turek, F. W. (2002). The effects of social defeat and other stressors on the expression of circadian rhythms. *Stress (Amsterdam, Netherlands)*, *5*(1), 15-22.
- Meijer, J. (2001). In Takahashi, J.S., Turek, F.W., & Moore, R.Y. (Eds.), *Handbook of Behavioral Neurobiology*, vol. 12 (pp. 183-222). New York: Kluwer Academic/Plenum.
- Meister, B., & Elde, R. (1993). Dopamine transporter mRNA in neurons of the rat hypothalamus. *Neuroendocrinology*, *58*(4), 388-395.
- Meister, B., Hökfelt, T., Vale, W. W., Sawchenko, P. E., Swanson, L., & Goldstein, M. (1986). Coexistence of tyrosine hydroxylase and growth hormone-releasing factor in a subpopulation of tubero-infundibular neurons of the rat. *Neuroendocrinology*, *42*(3), 237-247.

- Mistlberger, R. E. (1994). Circadian food-anticipatory activity: formal models and physiological mechanisms. *Neuroscience and biobehavioral reviews*, *18*(2), 171-195.
- Moore, R.Y., & Bloom, F.E. (1978). Central catecholamine neuron systems: anatomy and physiology of the dopamine systems. *Annu Rev Neurosci*, *1*, 129-169.
- Moore, R. Y., Speh, J. C., & Card, J. P. (1995). The retinohypothalamic tract originates from a distinct subset of retinal ganglion cells. *J. Comp. Neurol.*, *352*(3), 351-366.
- Nass, R., Hahn, M. K., Jessen, T., McDonald, P. W., Carvelli, L., & Blakely, R. D. (2005). A genetic screen in *Caenorhabditis elegans* for dopamine neuron insensitivity to 6-hydroxydopamine identifies dopamine transporter mutants impacting transporter biosynthesis and trafficking. *J Neurochem*, *94*(3), 774-785.
- Nestler, E. J., & Carlezon, W. A. (2006). The mesolimbic dopamine reward circuit in depression. *Biological Psychiatry*, *59*(12), 1151-1159.
- Nikaido, T., Akiyama, M., Moriya, T., & Shibata, S. (2001). Sensitized increase of period gene expression in the mouse caudate/putamen caused by repeated injection of methamphetamine. *Mol Pharmacol*, *59*(4), 894-900.
- Paxinos, G., & Watson, C. (2004). *The Rat Brain in Stereotaxic Coordinates* (Fourth ed.). New York: Elsevier.
- Pezük, P., Göz, D., Aksoy, A., & Canbeyli, R. (2006). BNST lesions aggravate behavioral despair but do not impair navigational learning in rats. *Brain Res Bull*, *69*(4), 416-421.
- Phelix, C. F., Liposits, Z., & Paull, W. K. (1992). Monoamine innervation of bed nucleus of stria terminalis: an electron microscopic investigation. *Brain Res Bull*, *28*(6), 949-965.
- Ralph, M. R., Foster, R. G., Davis, F. C., & Menaker, M. (1990). Transplanted suprachiasmatic nucleus determines circadian period. *Science*, *247*(4945), 975-978.
- Ramanathan, C., Nunez, A. A., Martinez, G. S., Schwartz, M. D., & Smale, L. (2006). Temporal and spatial distribution of immunoreactive PER1 and PER2 proteins in the suprachiasmatic nucleus and peri-suprachiasmatic region of the diurnal grass rat (*Arvicanthis niloticus*). *Brain Research*, *1073-1074*, 348-358.
- Ramanathan, C., Nunez, A. A., & Smale, L. (2008). Daily rhythms in PER1 within and beyond the suprachiasmatic nucleus of female grass rats (*Arvicanthis niloticus*). *Neuroscience*, *156*(1), 48-58.

- Redlin, U. (2001). Neural basis and biological function of masking by light in mammals: suppression of melatonin and locomotor activity. *Chronobiol Int*, 18(5), 737-758.
- Reppert, S. M., & Weaver, D. R. (2002). Coordination of circadian timing in mammals. *Nature*, 418(6901), 935-941.
- Resstel, L. B. M., Alves, F. H. F., Reis, D. G., Crestani, C. C., Corrêa, F. M. A., & Guimarães, F. S. (2008). Anxiolytic-like effects induced by acute reversible inactivation of the bed nucleus of stria terminalis. *Neuroscience*, 154(3), 869-876.
- Rey, P., Lopez-Real, A., Sanchez-Iglesias, S., Muñoz, A., Soto-Otero, R., & Labandeira-Garcia, J. L. (2007). Angiotensin type-1-receptor antagonists reduce 6-hydroxydopamine toxicity for dopaminergic neurons. *Neurobiol Aging*, 28(4), 555-567.
- Rivkees, S. A., & Lachowicz, J. E. (1997). Functional D1 and D5 dopamine receptors are expressed in the suprachiasmatic, supraoptic, and paraventricular nuclei of primates. *Synapse*, 26(1), 1-10.
- Rodríguez, M., Barroso-Chinea, P., Abdala, P., Obeso, J., & González-Hernández, T. (2001). Dopamine cell degeneration induced by intraventricular administration of 6-hydroxydopamine in the rat: similarities with cell loss in parkinson's disease. *Exp Neurol*, 169(1), 163-181.
- Roedter, A., Winkler, C., Samii, M., Walter, G. F., Brandis, A., & Nikkhah, G. (2001). Comparison of unilateral and bilateral intrastriatal 6-hydroxydopamine-induced axon terminal lesions: evidence for interhemispheric functional coupling of the two nigrostriatal pathways. *J. Comp. Neurol.*, 432(2), 217-229.
- Roybal, K., Theobald, D., Graham, A., DiNieri, J. A., Russo, S. J., Krishnan, V., et al. (2007). Mania-like behavior induced by disruption of CLOCK. *Proc Natl Acad Sci USA*, 104(15), 6406-6411.
- Rusak, B., Robertson, H. A., Wisden, W., & Hunt, S. P. (1990). Light pulses that shift rhythms induce gene expression in the suprachiasmatic nucleus. *Science*, 248(4960), 1237-1240.
- Schwartz, R. K., & Huston, J. P. (1996). Unilateral 6-hydroxydopamine lesions of meso-striatal dopamine neurons and their physiological sequelae. *Prog Neurobiol*, 49(3), 215-266.
- Segall, L. A., Perrin, J. S., Walker, C.-D., Stewart, J., & Amir, S. (2006). Glucocorticoid rhythms control the rhythm of expression of the clock protein, Period2, in oval nucleus of the bed nucleus of the stria terminalis and central nucleus of the amygdala in rats. *Neuroscience*, 140(3), 753-757.

- Sellix, M. T., Egli, M., Poletini, M. O., McKee, D. N. T., Bosworth, M. D., Fitch, C. A., et al. (2006). Anatomical and functional characterization of clock gene expression in neuroendocrine dopaminergic neurons. *Am J Physiol Regul Integr Comp Physiol*, 290(5), R1309-1323.
- Shibata, S., Hamada, T., Tominaga, K., & Watanabe, S. (1992). An in vitro circadian rhythm of protein synthesis in the rat suprachiasmatic nucleus under tissue culture conditions. *Brain Research*, 584(1-2), 251-256.
- Soler, R., Füllhase, C., Santos, C., & Andersson, K.-E. (2010). Development of bladder dysfunction in a rat model of dopaminergic brain lesion. *Neurourology and urodynamics*.
- Stephan, F. K. (2002). The "other" circadian system: food as a Zeitgeber. *J Biol Rhythms*, 17(4), 284-292.
- Stephan, F. K., & Zucker, I. (1972). Circadian rhythms in drinking behavior and locomotor activity of rats are eliminated by hypothalamic lesions. *Proc Natl Acad Sci USA*, 69(6), 1583-1586.
- Stocchi, F., & Brusa, L. (2000). Cognition and emotion in different stages and subtypes of Parkinson's disease. *J Neurol*, 247 Suppl 2, II114-121.
- Takahashi, S., Yokota, S., Hara, R., Kobayashi, T., Akiyama, M., Moriya, T., et al. (2001). Physical and inflammatory stressors elevate circadian clock gene mPer1 mRNA levels in the paraventricular nucleus of the mouse. *Endocrinology*, 142(11), 4910-4917.
- Takao, T., Tachikawa, H., Kawanishi, Y., Mizukami, K., & Asada, T. (2007). CLOCK gene T3111C polymorphism is associated with Japanese schizophrenics: a preliminary study. *Eur Neuropsychopharmacol*, 17(4), 273-276.
- Thornton, E., Tran, T. T. B., & Vink, R. (2010). A substance P mediated pathway contributes to 6-hydroxydopamine induced cell death. *Neurosci Lett*.
- Ungerstedt, U. (1971a). Stereotaxic mapping of the monoamine pathways in the rat brain. *Acta Physiol Scand Suppl*, 367, 1-48.
- Ungerstedt, U. (1971b). Adipsia and aphagia after 6-hydroxydopamine induced degeneration of the nigro-striatal dopamine system. *Acta Physiol Scand Suppl*, 367, 95-122.
- van den Pol, A. N., Herbst, R. S., & Powell, J. F. (1984). Tyrosine hydroxylase-immunoreactive neurons of the hypothalamus: a light and electron microscopic study. *Neuroscience*, 13(4), 1117-1156.

- van Vulpen, E. H., Yang, C. R., Nissen, R., & Renaud, L. P. (1999). Hypothalamic A14 and A15 catecholamine cells provide the dopaminergic innervation to the supraoptic nucleus in rat: a combined retrograde tracer and immunohistochemical study. *Neuroscience*, *93*(2), 675-680.
- Verwey, M., Khoja, Z., Stewart, J., & Amir, S. (2007). Differential regulation of the expression of Period2 protein in the limbic forebrain and dorsomedial hypothalamus by daily limited access to highly palatable food in food-deprived and free-fed rats. *Neuroscience*, *147*(2), 277-285.
- Volkow, N.D., Fowler, J.S., Wang, G.J., Swanson, J.M., Telang, F. (2007). Dopamine in drug abuse and addiction: results of imaging studies and treatment implications. *Arch Neurol*, *64*(11), 1575-1579.
- Weaver, D.R., & Reppert, S.M. (1995). Definition of developmental transition from dopaminergic to photic regulation of *c-fos* gene expression in the rat suprachiasmatic nucleus. *Mol Brain Res*, *33*, 136-148.
- Weaver, D. R., Rivkees, S. A., & Reppert, S. M. (1992). D1-dopamine receptors activate *c-fos* expression in the fetal suprachiasmatic nuclei. *Proc Natl Acad Sci USA*, *89*(19), 9201-9204.
- Weiner, D. M., Levey, A. I., Sunahara, R. K., Niznik, H. B., O'Dowd, B. F., Seeman, P., et al. (1991). D1 and D2 dopamine receptor mRNA in rat brain. *Proc Natl Acad Sci USA*, *88*(5), 1859-1863.
- Welsh, D. K., Logothetis, D. E., Meister, M., & Reppert, S. M. (1995). Individual neurons dissociated from rat suprachiasmatic nucleus express independently phased circadian firing rhythms. *Neuron*, *14*(4), 697-706.
- Woelfle, M. A., Ouyang, Y., Phanvijhitsiri, K., & Johnson, C. H. (2004). The adaptive value of circadian clocks: an experimental assessment in cyanobacteria. *Curr Biol*, *14*(16), 1481-1486.
- Yamada, N., & Martin-Iverson, M. T. (1991). Selective dopamine D1 and D2 agonists independently affect different components of the free-running circadian rhythm of locomotor activity in rats. *Brain Research*, *538*(2), 310-312.
- Yuferov, V., Kroslak, T., Laforge, K.S., Zhou, Y., Ho, A., & Kreek, M.J. (2003). Differential gene expression in the rat caudate putamen after "binge" cocaine administration: advantage of triplicate microarray analysis. *Synapse* *48*, 157-169.
- Zheng, B., Larkin, D. W., Albrecht, U., Sun, Z. S., Sage, M., Eichele, G., et al. (1999). The *mPer2* gene encodes a functional component of the mammalian circadian clock. *Nature*, *400*(6740), 169-173.

Zuch, C. L., Nordstroem, V. K., Briedrick, L. A., Hoernig, G. R., Granholm, A. C., & Bickford, P. C. (2000). Time course of degenerative alterations in nigral dopaminergic neurons following a 6-hydroxydopamine lesion. *J. Comp. Neurol.*, 427(3), 440-454.